Joint Centre for Mesoscale Meteorology, Reading, UK

Results from simulations of an organised convective event using the New Dynamics at 12, 4 and 2km resolution

N. Roberts

Internal Report No. 126
NWP Technical Paper No. 344

January 2001

Met Office Joint Centre for Mesoscale Meteorology Department of Meteorology
University of Reading PO Box 243 Reading RG6 6BB United Kingdom
Tel: +44 (0)118 931 8425 Fax: +44 (0)118 931 8791
www.metoffice.com

Designed and produced by the Met Office © Crown copyright 2001 01/0240 The Met Office logo is a registered trademark.

Results from simulations of an organised convective event using the New Dynamics at 12, 4 and 2km resolution

Nigel Roberts
Mesoscale Modelling Group, JCMM

January 2001

Abstract

With the development of the semi-implicit, semi-lagrangian, non hydrostatic formulation of the dynamics core of the Unified Model (the New Dynamics) comes the opportunity to run forecasts at much higher resolution than currently used. The Mesoscale Modelling group at the Joint Centre for Mesoscale Meteorology (JCMM) is currently involved with assessing the performance of the New Dynamics at high resolution. One aspect of this is an investigation into how well the model can simulate the type of organised convective storms that are associated with upper-level potential vorticity anomalies and can on occasion produce severe weather events.

The New Dynamics was run with 12, 4 and 2km horizontal resolution and 45 vertical levels for a case of intense organised convection on 2-3rd July 1999. This event was originally well forecast by the operational Unified Model and therefore made a good test case because the larger-scale dynamical forcing was well captured. All simulations were compared with observations. The effect of increasing the resolution was examined. The impact of changing the CAPE closure timescale in the convection scheme was investigated along with the the effect of running without the convection scheme. At 4km resolution the sensitivity to changing the length of the timestep was also examined.

The simulations showed a large sensitivity to changing the CAPE closure timescale for each of the resolutions. A curious interaction between the dynamics and the convection scheme was observed when the CAPE closure timescale was sufficiently short. When the convection scheme was switched off the storms became more organised and squall lines developed at 4 and 2km resolution. The propagation speed of the storm line increased with increasing resolution. The best simulation was the 2km run without the convection scheme.

Contents

1. Introduction 1
2. Observations 2
   2.1 The event 2
   2.2 Quantitative measurements from the observations 4
   2.3 The large-scale mechanism and choice of case study 4
3. Performance of the operational mesoscale model 5
4. Setting up the New Dynamics (ND) runs 7
   4.1 The domains 7
   4.2 Settings 8
5. An initial look at ND runs at 12 and 4km resolution 9
6. The sensitivity to changing the CAPE closure timescale (CCT) 11
   6.1 What is the CAPE closure timescale(CCT) 11
   6.2 Why run with convective parametrization at high resolution 12
   6.3 12km resolution forecasts 13
   6.4 4km resolution forecasts 14
   6.5 2km resolution forecasts 15
   6.6 The variation in average rainfall rates 16
   6.7 The variation in peak rain rates 17
   6.8 Key results from varying the CCT 18
7. Unrealistic convective rainbands 20
   7.1 Description of the rainbands in a 4km run with a 30-minute CCT 21
   7.2 A probable mechanism 22
   7.3 The effect of switching off the convection scheme after 6 hours 25
   7.4 Summary of this section 25
8. Changing the timestep at 4km resolution 26
9. Running without the convection scheme 29
   9.1 Summary of this section 33
10. Meteorological assessment of forecast performance 34
   10.1 Propagation speed of the storms 34
   10.2 Peak rainfall intensity 37
   10.3 The organisation of the storms 38
11. Conclusions 39
   11.1 Future work 39
   11.2 Acknowledgements 40
12. References 40

Appendix 1 Details about the domains used 41
Appendix 2 General settings used in the model runs 41

1. Introduction

The semi-implicit, semi-lagrangian, non hydrostatic formulation of the dynamics core of the Unified Model (the New Dynamics (ND)) has now been developed (Staniforth et al 2000) and will soon become operational. One of the important features of the ND is that because it is non-hydrostatic it can deal with vertical accelerations and will in principle allow us to run the model at very high resolution (down to order 1km or better). The potential benefits of being able to run a forecast model routinely at much higher resolution are enormous. Many more mesoscale weather events can be properly resolved and local effects much better simulated. This in turn should result in substantially improved forecasts and lead to new and improved products for our customers. The drawback is that higher resolution is more costly, in both computer time and memory. We have to be sure that the benefit outweighs the cost. The skill of high-resolution forecasts may sometimes be largely dependent on what comes in through the boundaries with the extra resolution only acting to amplify existing errors or produce spurious detail.

The Mesoscale Modelling group at the Joint Centre for Mesoscale Meteorology (JCMM) is currently involved with assessing the performance of the New Dynamics at high resolution. One aspect of this is an investigation into how well the model can simulate organised convection at high resolution. There are several reasons for being interested in this phenomena.

1. Organised thunderstorms produce severe weather and are identified as an area of particular concern by users.
2. Higher resolution should improve the representation of these events.
3. The role of the convection scheme at high resolution needs to be investigated.
4. Rapid development and large vertical velocities present a challenge.
5. Organised convection associated with upper-level potential vorticity (PV) anomalies presents a more difficult forecasting problem than local convection because the evolution of the PV anomaly is crucial.

The aim of this report is to present some preliminary results from 12, 4 and 2km simulations of an organised convective event that occurred on the 3rd July 1999. This event was chosen because the operational forecast was good. The extra detail from the higher resolution could be assessed without too much concern about the synoptic-scale accuracy.

Topics covered are:

- The impact of increasing the resolution.
- The sensitivity to changing the CAPE closure timescale in the convection scheme.
- Propagating bands of rain from the convection scheme that degraded the forecast accuracy.
- The results from running without the convection scheme.
- The impact of changing the length of the timestep.
- Assessment of the forecasts against observations.

2. Observations

2.1 The event

Severe thunderstorms developed over Wales and southern England in the late evening of 2nd July 1999 and tracked east-northeast to clear away from the eastern coast of England by 0700 on the 3rd. The precipitation was very intense in places, with 44mm falling in less than 1 hour in Reading and more than 50mm falling at Heathrow Airport. Most of the rain at Reading fell in a 20 minutes period as rain rates exceeded 100mm/hr causing local flooding of homes. Ahead of the most severe storms, bands of precipitation from medium-level convective cloud gave mainly light precipitation but some lightning.

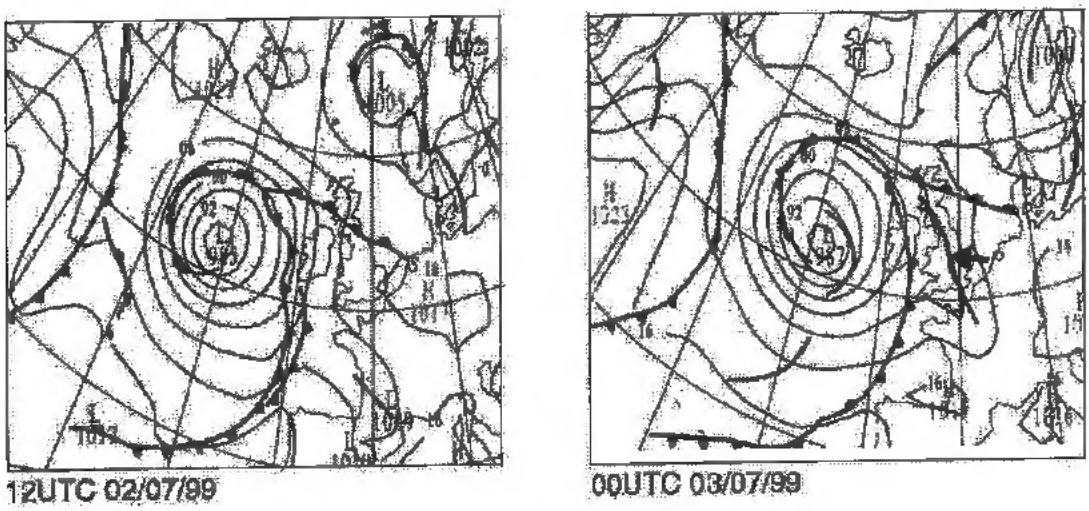

Figure 1. Mean Sea Level Pressure and frontal analysis of the synoptic situation.

The synoptic situation is shown in Figure 1. The UK was under the influence of a warm southerly flow on the eastern side of a low-pressure centre located to the west of Ireland. The thunderstorms occurred ahead of the surface cold front along an upper-level trough, analysed as a line with open triangles to the south-west of the UK on the 12UTC chart, which then became the line drawn down the spine of the UK on the 00UTC chart.

Figure 2 shows the rapid growth of the upper-level cold cloud shields generated from the two primary areas of deep convection indicated by the arrows. By 0300UTC on 3rd July the area covered by cloud at a temperature below -45C had grown to around 75000km^2 as the two cloud shields merged.

The radar sequence in Figure 3 shows the organisation and track of the two main precipitation regions. Rainfall rates averaged over the 5x5km squares displayed often exceeded 32mm/hr (though errors in quantitative radar measurements may be as high as 50% - A.J. Illingworth private communication). Between 00UTC and 03UTC the size and intensity of the rain areas did not change much as they progressed eastward, but the southern area became more organised and formed a squall line structure. The bands of lighter precipitation that developed earlier and ahead of the two main storm regions came from the mid-level altocumulus convection.

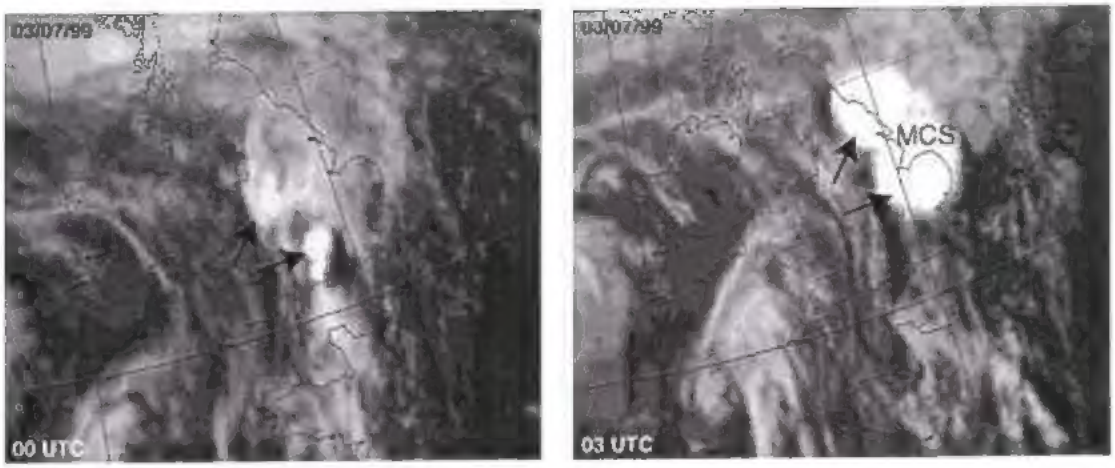

Figure 2. Meteosat Infrared images for 00 & 03 UTC 3/7/99. White/light shades show the highest and coldest cloud. Darker/darkest shades show low and warm cloud or the land/sea surface. The arrows point to the two main storm regions. MCS refers to Mesoscale Convective System.

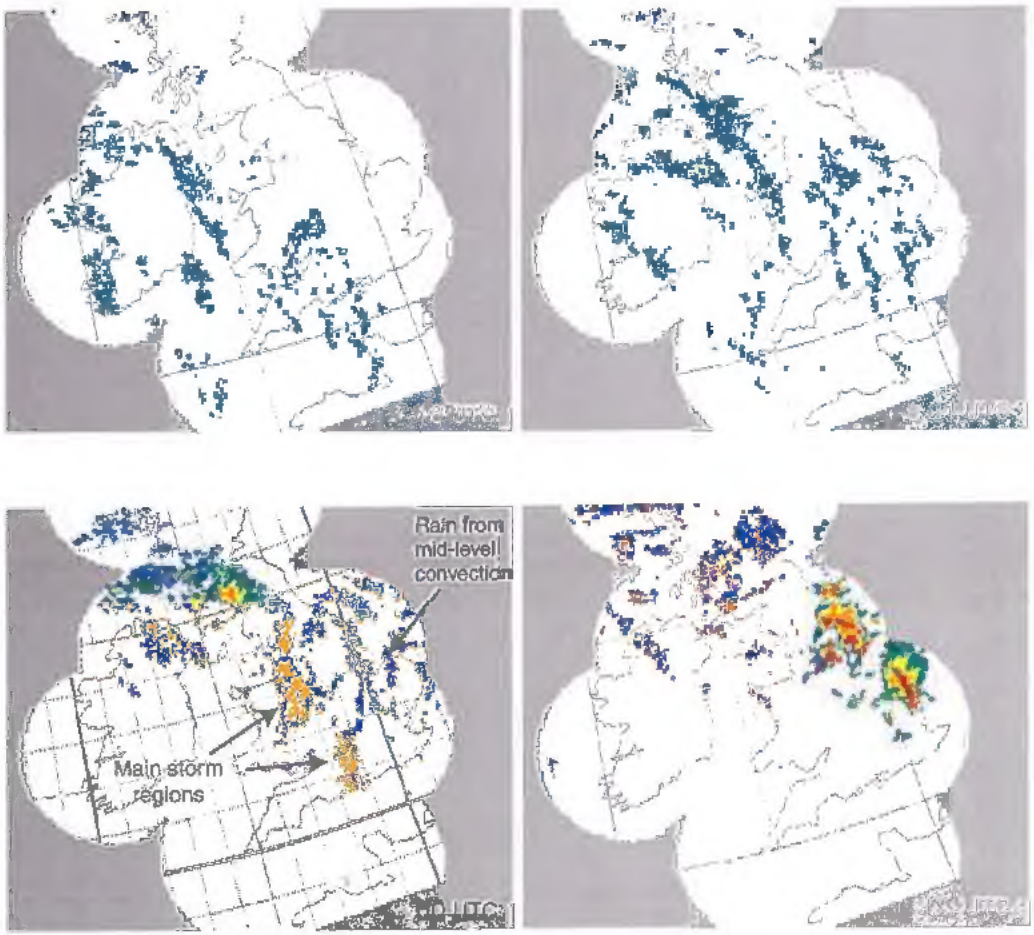

Figure 3. Network radar images for 18, 21UTC 2/7/99 and 00, 03UTC 3/7/99 at 5km resolution. Rainfall rates (mm/hr) are: blue <0.5, dark green 0.5–1, blue/green 1–2, yellow 2-4, orange 4-8, red 8-16, dark red/brown 16-32, light green 32-64. Highest intensities are 32-64mm/hr.

2.2 Quantitative measurements from the observations

The measurements listed below in Table 1 have been included because they have been used in quantitative assessment of model simulations and some will be referred to later. The maximum rain rate at Reading comes from a tipping siphon rain gauge at the Reading University site. The calculation of the estimated vertical velocity over the southern rain area assumes a steady state system between 00 and 02UTC. The rain region size is assumed to be a constant average over the period. The vertical velocity is based on the rate of anvil expansion over the 2-hour period for the constant rain area assuming an anvil depth of 1 or 2km.

Start time of northern storm area (nearest half hour)	21UTC 2/7/99
Start time of southern storm area (nearest half hour)	23UTC 2/7/99
Average maximum precipitation rates	50mm/hour
Maximum rain rate at Reading	160mm/hr +/- 50
Anvil size at 00 UTC (southern storm)	6800km^2
Anvil size at 02 UTC (southern storm)	26100km^2
Rate of anvil expansion	9650km^2/hour
Rain region size at 00UTC (southern storm)	6200km^2
Rain region size at 02UTC (southern storm)	10300km^2
Estimated mean vertical velocity over southern rain area	0.5 - 1.0 m/s $^+$/. 0.3
Propagation speed & direction of storms	67km/hr $^+$/. 3, 228 deg $^+$/. 2
Speed of the forward edge of the dry area in WV imagery	68km/hr $^+$/. 4
Width of narrow rainband at 03UTC	15-20km
Coldest cloud top temperature (from IR imagery)	-65C
Surface θ_w ahead of the surface cold front	17-19C
Surface θ_w behind the surface cold front	14-15C
The θ_w of the mid-level over-running air	14-15C
The θ_w of the boundary-layer air	17-19C

Table 1.

2.3 The large-scale mechanism and choice of case study

Thunderstorms often develop along the leading edge of dry (high brightness temperature) regions observed in water vapour (WV) imagery (Roberts 2000). The case being studied was chosen because it clearly developed in this way (Figure 5b) and as a result we can make deductions about the larger-scale forcing. A dry zone in WV imagery is usually an indication of a local lowering of the tropopause and therefore a positive potential vorticity (PV) anomaly in the upper troposphere. The thunderstorms were triggered as low-θ_w air at middle levels was advected around the southern flank of the upper-level PV anomaly and overran the higher-θ_w air at lower levels advecting northward over the UK. Vertical motion ahead of the PV anomaly and associated with the low-level warm advection provided a means of destabilising the atmosphere sufficiently to allow a release of the potential instability generated by the overrunning process. This triggering mechanism was deduced on the basis of a synthesis of observations, imagery, and NWP model diagnostics combined with knowledge of similar events (Browning & Roberts 1996, Roberts 2000) and the use of PV ideas (Hoskins et al 1985, Griffiths et al 1998). A detailed description of the event will not be given here.

The major advantage of choosing a case study in which the large-scale forcing is largely understood is that it is then possible to separate the large-scale dynamics from the

convective scales when assessing the performance of a numerical model forecast. We can concentrate on the model's representation of convection in relation to its own large-scale dynamical forcing rather than say geographical location. (Large scale in this context means the dynamics resolved over several grid points or more in the initial fields or advected through the boundaries during the forecast). The accuracy of the large-scale forcing in high-resolution model simulations is essentially an issue of data assimilation in the driving model and not the focus of this report. It follows, that an ideal test case for assessing the representation of organised convection is one in which the large-scale forcing in the model is close to that observed – this case is good in that respect, as will be shown.

3. Performance of the operational mesoscale model

The operational mesoscale configuration of the Unified Model (UM) was re-run from a nominal analysis time of 12UTC 2/7/99. This included data assimilation using the AC scheme between 09 and 14UTC. Figures 4 and 5 show output from this run compared with observations.

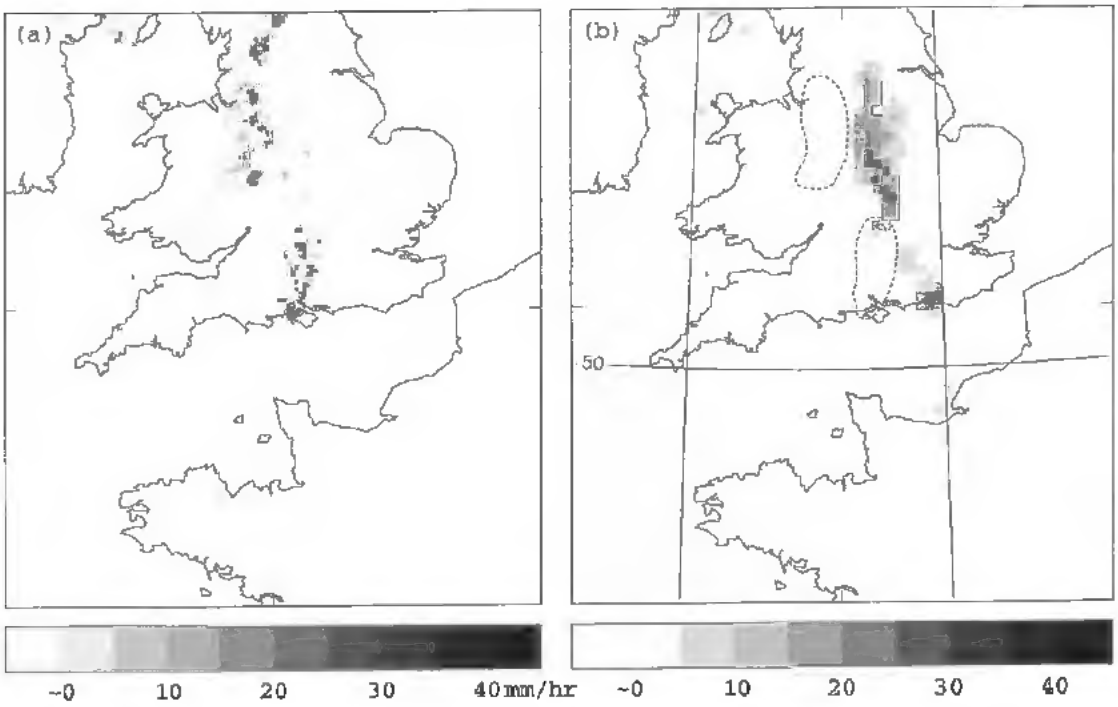

Figure 4. 00UTC 3/7/99 Precipitation rates. (a) NIMROD composite radar picture. (b) Total precipitation rate from a 12 hour forecast from the Unified Model operational mesoscale configuration re-run. The area shown is a sub-area of the re-run domain to match the radar picture. The dashed lines enclose the main precipitation areas in (a).

Figure 4 shows that the model did produce precipitation in approximately the correct position with approximately the correct intensity. A good forecast given the propagation speed of the storms (67 km/hr), but with some errors nevertheless. At 00UTC the model's precipitation regions were 80km too far east and 50km too far south, the mid-level convection ahead of the main rain areas was not captured by the model and the convective precipitation over NE France was probably not correct.

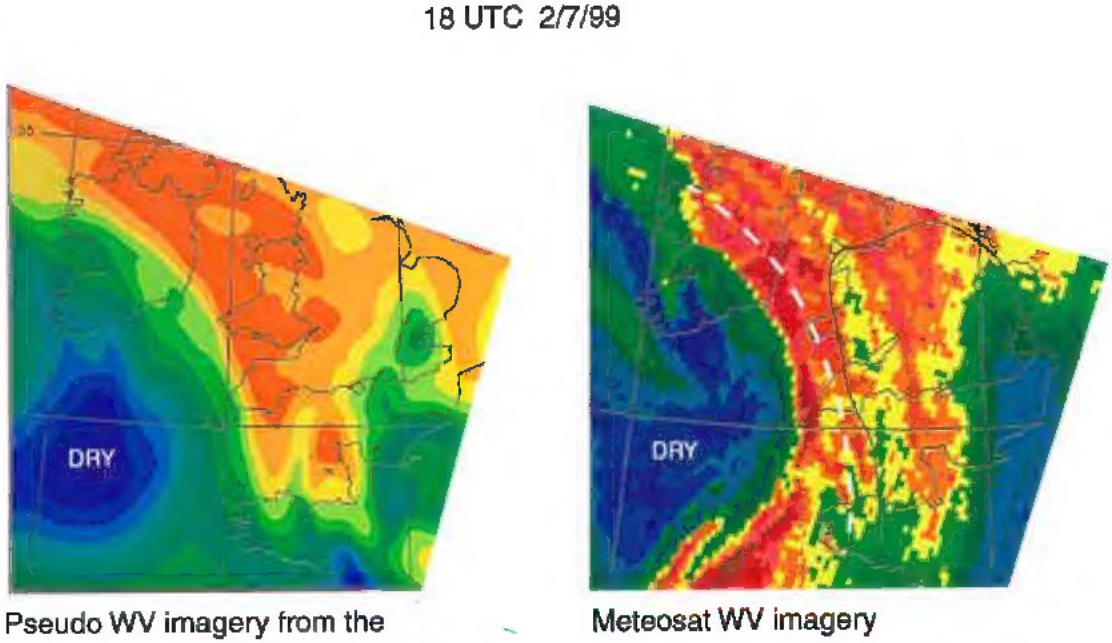

Figure 5. (a) An equivalent to the Meteosat water vapour channel calculated from operational mesoscale model fields for a six hour forecast valid at 18 UTC 2/7/99. Blues-greens represent dry air above 600hPa; yellows-oranges represent moist air or cloud above 600hPa. (b) Meteosat water vapour image for 18 UTC 2/7/99. The colour trends are the same as (a) but the colour scales are different. The white dashed line marks the leading edge of the dry air in (a). The black line encloses the warm tongue of high θ_w air at the surface derived from surface observations.

A good way of finding out how well a forecast matches the real atmosphere in the upper troposphere is by a comparison of pseudo WV imagery from model fields with satellite WV imagery. Such a comparison is especially useful for this type of case with an obvious isolated dry region. Figure 5 reveals a generally good match between the model and the imagery; both have a dry region (blue) to the south of Ireland and a band of cloud/moist air through SW England, Wales through to the North of the Republic of Ireland and Northern Ireland. This indicates that the larger-scale upper-tropospheric dynamics of the model fitted reasonably well with reality and so the rainfall prediction was close to that observed for the right reasons. As with the rainfall comparison, there are some significant differences. The forward edge of the dry region in the model was more advanced than in the satellite imagery (fitting with the more advanced rainfall). The model did not have the same curvature in the pattern – there should have been cloudiness/moisture to the west of France and there was not.

Low levels were important too. Wet-bulb potential temperature at 950hPa from the model was compared with surface observations (not shown) to detect any error in the position of the surface cold front. It turns out that the model-forecast position of the cold front was excellent in the early stages, but somewhat poorer over the English Channel later.
In summary, the mesoscale configuration of the UM produced a good representation of the observed large-scale dynamics and because of this can provide a good initial state for New Dynamics sensitivity experiments. Differences from the observed pattern at early times can be related to errors in the precipitation forecast later.

4. Setting up the New Dynamics (ND) runs

4.1 The domains

Experiments using the New Dynamics (ND) (Staniforth 2000) have been run with horizontal resolutions of 12, 4 and 2km. The three domains used for these horizontal resolutions are shown in figure 6 and called D12, D4 and D2. This choice was largely one of convenience as this was a first attempt to run at such high resolution for an intense convective event over the UK. D12 was used because it is the same as the UM mesoscale domain so the ancillary files already existed and a direct comparison against the UM could be made. D4 was made small enough to run on 64 processors in less than 5000 seconds on t3ea but still large enough to capture the evolution of the storms. D2 was made as large as possible without being too close to the edge of D4. In fact, the edge of D2 was close to the edge of D4 (Figure 6) and this was not ideal. However, most of the convective scale development occurred within the domain(s) away from the boundaries and it was hoped that this would make the adjacency of the D4 & D2 boundaries less of an issue.

It is arguable that domains extending further west may have been preferable for this specific case (and in general), but given the constraint of starting with the UM mesoscale area this set-up is a good starting point for future work. An additional benefit is that the Chilbolton doppler radar is located at the centre of D4 and D2; ideal for verification of precipitating regions in further case studies.

The number of vertical levels used was either 38 or 45 (Lean 2000). Most of the results shown in this report come from 45 level simulations because that seemed more appropriate with very high horizontal resolution, but the sensitivity to vertical resolution does require further assessment. Further details about the domains used are given in appendix 1.

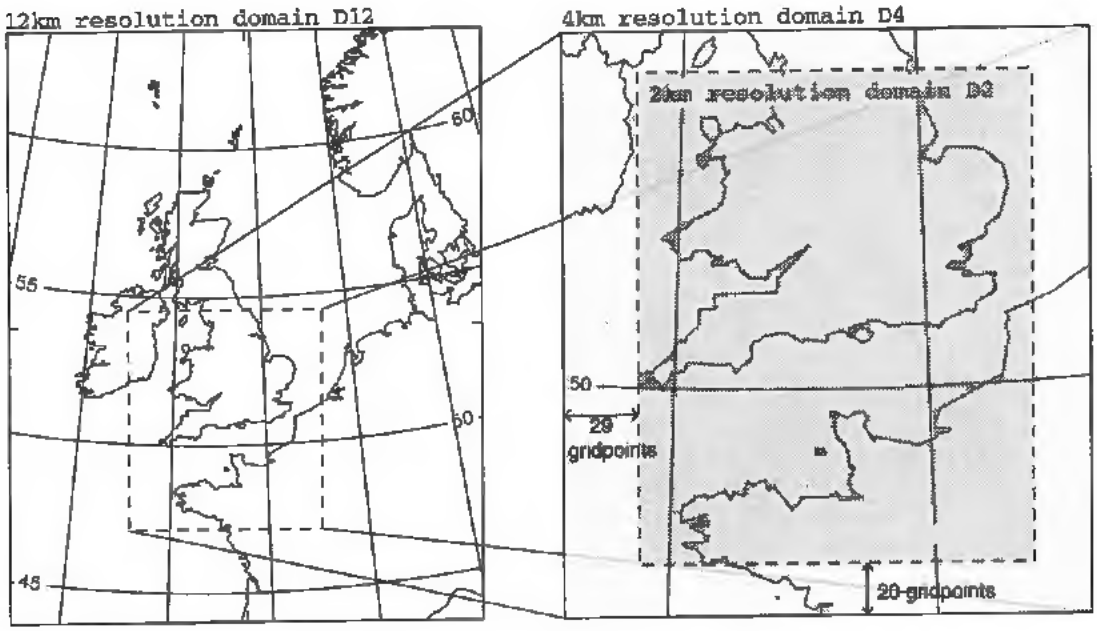

Figure 6. The three domains used for New Dynamics simulations.

4.2 Settings

The ND could not be run with data assimilation because at the time these experiments were run that capability was not available. The best way to include data assimilation was to run the UM from 09 to 15UTC 2/7/99 then run the ND from 15UTC. Starting the runs at an earlier time would have made the forecast period too long, starting at a later time would not have allowed enough spin up time before the storms developed. Another solution might have been to run the ND from 12UTC and only have the first three hours of the data assimilation in the UM but this produced a measurable degradation in the forecast.

Figure 7 shows a schematic of the set-up of the runs. The UM was run on a global domain from 09 to 15UTC 2/7/99 with assimilation of 3D VAR analysis. The fields at 15UTC were then reconfigured to the ND grid and the ND run forward on a global domain to 03UTC 3/7/99.

The UM was also run on the standard mesoscale domain from 09 to 15UTC with data assimilation using the AC scheme up to 14UTC and boundary updating every 3 hours from the UM global run. The UM mesoscale fields at 15UTC were then reconfigured to the ND mesoscale 12km resolution grid and the ND was run forward to 03UTC 3/7/99 with boundary updating every 3 hours from the ND global run. The 4km and 2km resolution ND runs were also started at 15UTC from a reconfiguration of the mesoscale UM run and run to 03UTC 3/7/99. The ND 4km resolution run had boundary updating every hour from the ND 12km run and the ND 2km run had boundary updating every hour from the ND 4km run.

The timesteps used for the high-resolution ND integrations were 5, 2, 1 minute(s) for the 12, 4, 2km resolution runs respectively. A radiation scheme timestep of 1 hour was used for the 12km runs and 20 minutes for the 4 and 2km runs. The ancillary fields were generated using the ancillary creation program version 5.0. The orography was derived from a 2km-resolution orography dataset which had been derived (Ian Culverwell) from the raw 100m- resolution DTED dataset. Orography at the boundaries was merged linearly over 4 gridpoints between that on the model grid and that on the coarser resolution grid of the run providing the boundary updates. The ND integrations described in this report were run from either version 2.9 or mostly from version 3.0 of the New Dynamics. This used the script system available before the Unified Model User Interface (UMUI) was ready for ND simulations. Please see acknowledgements. More information about the high resolution ND set-up used is given in appendix 2.

Some problems did occur initially. The first 4km resolution run failed after timestep 8. A change in the diffusion from del 2 to del 4 with a coefficient of 6.8e3 enabled the run to succeed. These changes were recommended (P A Clark) to alleviate problems associated with deep valleys in the high-resolution orography dataset in previous attempts to run at 4km. The global ND failed at the start of the run. A reduction in the timestep from 15 minutes to 10 minutes solved this. The introduction of data assimilation may allow a return to a longer timestep because of a more balanced initial state.

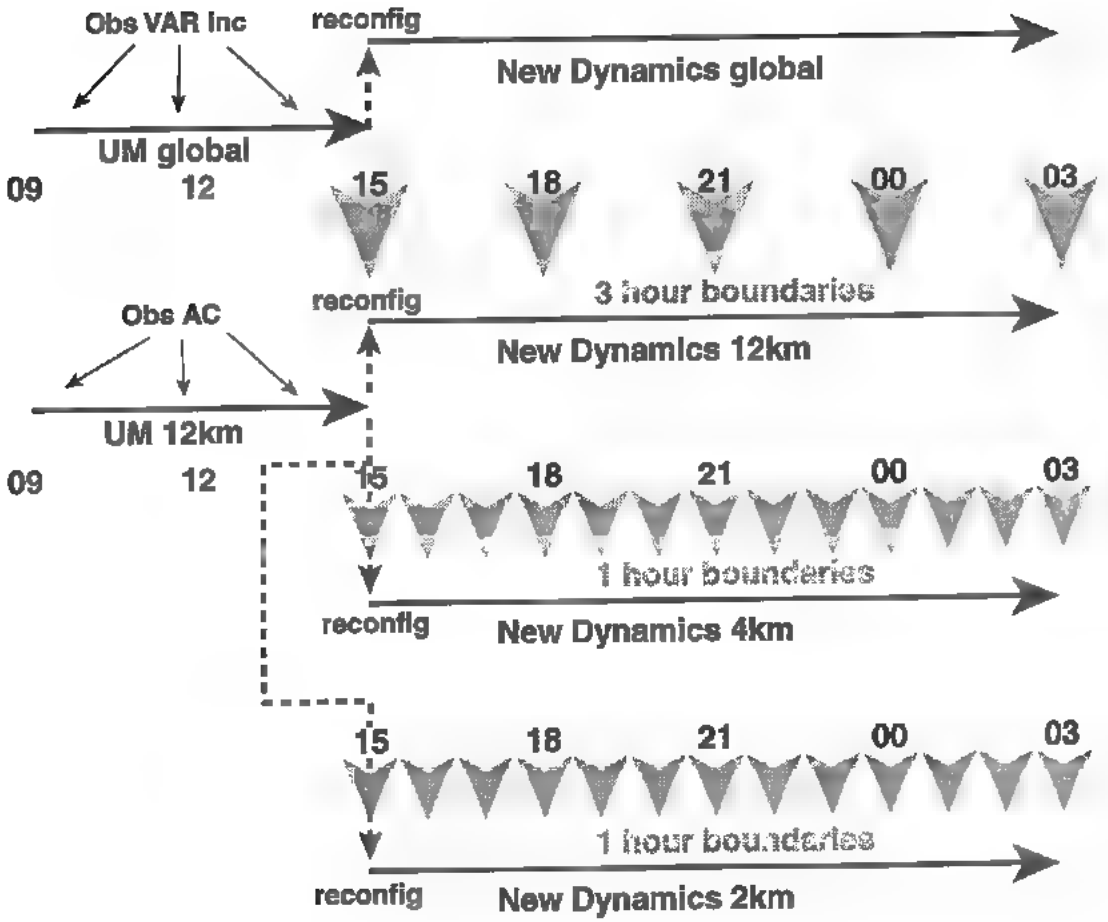

Figure 7. A schematic of the set-up of the New Dynamics runs. Further description in the text.

5. An initial look at ND runs at 12 and 4km resolution

It is not an aim of this report to make a direct comparison between the performance of the ND and the UM. There are several reasons for this; firstly, the ND is at an immediate disadvantage until data assimilation is introduced - when this happens direct comparisons will be made; secondly, the optimal physics settings are likely to be different for the ND compared to the UM and this requires investigation beyond work done so far; thirdly, a primary aim of this project is to assess the capability and performance of high resolution (4 and 2km) simulations.

Nevertheless, it is important to get a view of the ND performance compared with the UM, so that general concerns can be introduced before plunging into detail. Figure 8 shows output from UM and ND simulations at 12km resolution and a ND simulation at 4km resolution. This UM run (a) is not the same as the UM re-run shown in Figure 4. Here, the convection scheme was run with CAPE closure rather than an adjustment closure (Gregory et al 1999) and the soil moisture was different. These changes were made to be directly comparable with future ND simulations. All the runs had a CAPE closure timescale of 30 minutes. Sensitivity to the CAPE closure timescale is covered in the next chapter. A major difference between the ND runs and the UM run was the number of vertical levels - 45 levels rather than 38. It turns out that the extra levels made little difference to the ND 12km run and it was considered better to use 45 levels for higher resolution simulations.

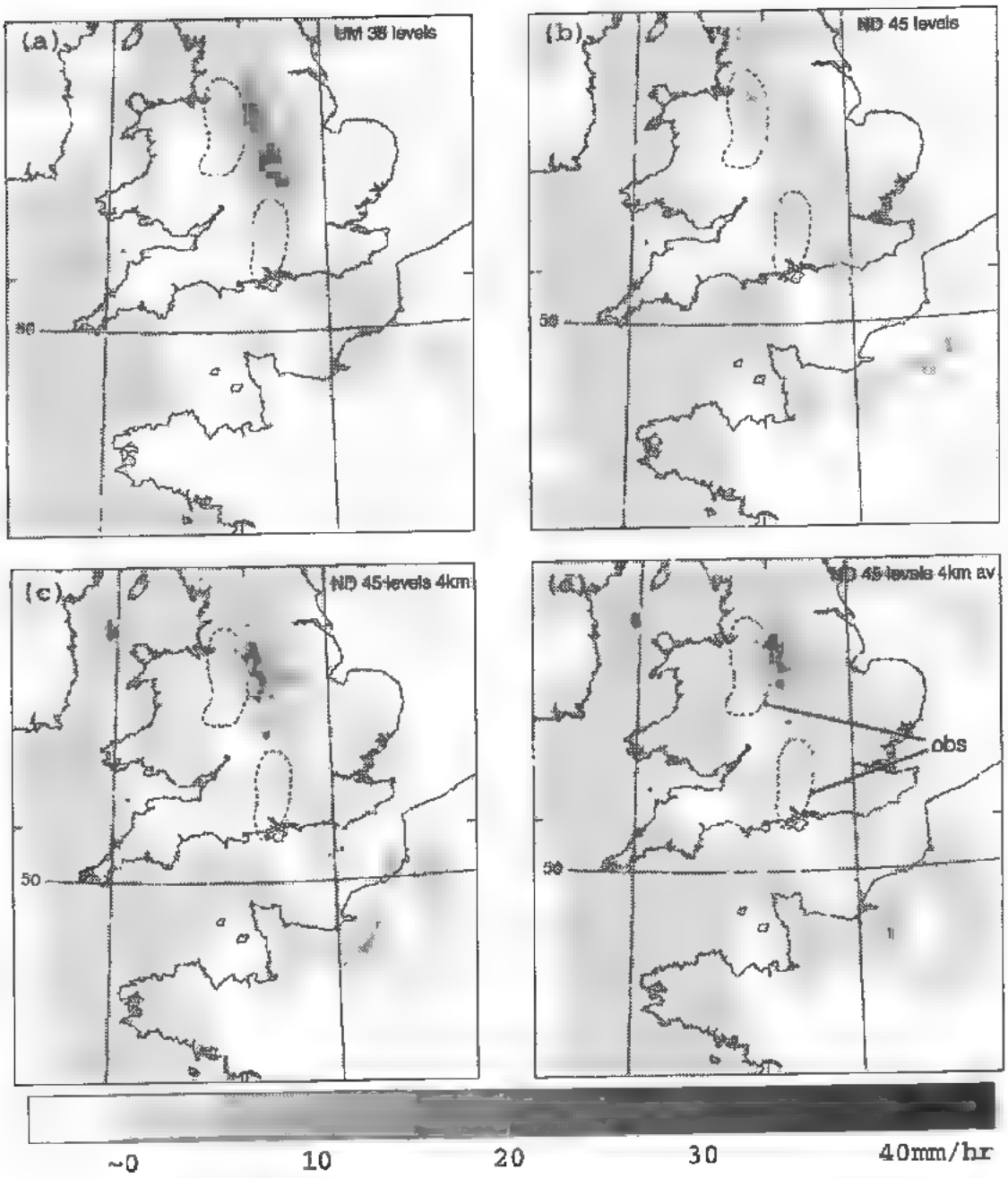

Figure 8. Total precipitation rates at 00UTC 3/7/99 from UM and ND model simulations. All begin with the same UM run from 09UTC to 15UTC 2/7/99 with data assimilation. All have a CAPE closure timescale of 30 minutes in the convection scheme. The dased lines enclose the main rain areas observed from radar. (a) Further 9 hours forecast with the UM at 12 km resolution using 38 vertical levels. (b) Further 9 hours forecast with the ND at 12km resolution using 45 levels. (c) Further 9 hours forecast with the ND at 4km resolution using 45 levels. (d) An average of (c) to 12km resolution.

Figure 8 shows a considerable difference in precipitation intensity between the 12km resolution UM (a) and ND (b) forecasts even though the mean sea level pressure fields were very similar (not shown). The UM had higher, more realistic, rain rates over central England which came mostly from the resolved precipitation rather than the convective; the ND had much lower rain rates and most of this came from the convection scheme. The precipitation covered roughly the same area, but the ND developed heavier rain out of the convection scheme over NE France (discussed later). Neither run produced the mid-level convective precipitation that was observed to the east of the main band.

The 4km resolution ND run (Figure 8c) developed more intense, more organised and finer structured precipitation than the 12km ND run (8b). The picture resembles the radar (Figure 4) in 'texture' but with positional errors. Whereas nearly all rain in the ND 12km run came from the convection scheme, the higher precipitation rates in the ND 4km run came mostly from the resolved dynamics. This is not a surprise, but even so, the degree of change in the rain rates is striking. There is a hint of an organised rain band over the North Sea, though without any significant improvement in the prediction of mid-level convection. The unrealistic convective precipitation over NE France still formed and was more organised than at 12km.

The amount of detail represented in the 4km simulation is considerable and whether the location of each individual storm cell is to be believed is doubtful. Averaging to coarser resolution has the benefit of removing some of the random sensitivity element of a forecast as well as providing a direct comparison with coarser resolution runs. The direct comparison of the ND 4km run averaged to 12km (8d) with the ND 12km run (8b) clearly shows that the 4km run has added value to the forecast even when degraded to 12km resolution. This 4km-resolution forecast is encouraging.

6. The sensitivity to changing the CAPE closure timescale (CCT)

This section discusses the impact of varying the CCT in the convection scheme (Gregory et al 1999) on the precipitation forecasts from the ND runs at 12, 4 and 2km resolution. The motivation for this comes from the need to find the most suitable CCT for each resolution (if possible), but only provided that the convection scheme behaves sensibly. Results from UM mesoscale simulations of this event revealed a huge sensitivity.

6.1 What is the CAPE closure timescale (CCT)

The CCT is defined as the timescale over which the Convectively Available Potential Energy (CAPE) in an atmospheric profile is reduced to zero and is used in the calculation of the cloud base mass flux, see equation 1. A shorter/longer CCT should result in stronger/weaker convection initially, but how this might feedback on to the dynamic fields' then further convection and ultimately forecast performance is not clear. It has been suggested that the CCT should be shortened with higher resolution to cope with potentially large vertical velocities. On the other hand, going to higher resolution means that convection is better resolved in the model dynamics and wiping out the instability with the convection scheme may not be sensible. It may be of course, that the best forecast is produced when the convection scheme is switched off.

$$M_B^{new} = \frac{CAPE}{\tau \sum_{cloud} [\, (1 + c_{vir}\, q^E\, Q1') + c_{vir}\, \theta^E\, Q2' \,] \frac{\Delta p}{\rho}} \qquad (1)$$

M_B^{new} is the adjusted cloud base mass flux, τ is the CAPE closure timescale, q^E and θ^E are the mixing ratio and potential temperature of the environment, Q1' and Q2' are the calculated rates of change of q and θ scaled by the original cloud base mass flux. See Gregory et al 1999.

6.2 Why run with convective parametrization at high resolution

Before just ploughing on, it is worth thinking about whether it makes scientific sense to run at high resolution with the convection scheme by considering the nature of the problem. The following is based on ideas by G. C. Graig and P. A. Clark (Private communication).

We are not yet in a position to be able to say at what resolution the performance of the model will be generally better without a convection scheme – perhaps at 8km, probably but not necessarily at 1km. Apart from anything else, the definition of 'better' is not trivial and may be largely dependant on the particular information that is required from a forecast as well as the method of validation.

The scales determined (or 'filtered') by the convection scheme should be an inherent characteristic of the convection scheme alone and NOT dependent on the discretization of the numerical model. This filter scaling is probably dependent on the CCT. A shorter CCT produces stronger convection which increases the speed of vertical exchange, destroys small scales more effectively and introduces more vertical diffusion into the solution. The discretization of the numerical solution determines the accuracy with which the 'dynamics+convection scheme' problem can be solved (assuming the scheme is well behaved – which it might not be). An ever-finer grid and shorter timestep should take the solution towards the continuous solution but never quite converge there.

Consider three scenarios:

1. Run with the convection scheme and a very short CCT.
   - The convection scheme does nearly all of the work; therefore as Δx decreases the solution (in convectively unstable regions) eventually has long scales compared to the gridlength and timestep. In effect, this solution is an ensemble average and little benefit is gained from high resolution, but we would expect runs with different resolutions to converge to the same solution before $\Delta x \Longrightarrow 0$ (if the convection scheme is well behaved).

2. Run with NO convection scheme.
   - All the convection is explicitly resolved, but the scales are determined by the numerical viscosity and therefore the resolution of the grid. Runs with different resolutions will not represent the same solution, although for the sake of the problem we are trying to solve they should converge at very high resolutions. Fine detail in the solution could be misleading as this is a single realisation of the scenario 1 ensemble and as such the individual elements of the solution have a degree of stochastic behaviour.

3. In between - Run with the convection scheme and some chosen CCT
   - Some of the convection is explicitly resolved. There is a dependence on the resolution and the filter scale of the convection scheme that results in a mixture of large scale averaging and a random element. More of the convection is explicitly resolved (and therefore dependant on the discretization) as the CCT gets longer or the grid gets finer. Runs with different resolutions may converge if the scales represented are longer than the smallest resolved by the grid. If those scales become much longer then scenario 1 is approached, if those scales are shorter then scenario 2 is approached.

This implies that it is reasonable to test runs at high resolution with a convection scheme, but the scales represented by the solution may (or should) be larger than the smallest representable by the grid. If there is then some kind of numerical convergence, it makes sense to run the model with only just enough resolution to represent these scales. What

these scales actually are and how they vary with CCT is not known to start with and must be found by experiment. The appropriate scale at which to make comparisons with observations is then established.

6.3 12km resolution forecasts (see Figure 9)

As expected, changing the CCT had a significant impact on both the distribution and intensity of precipitation in the 12km resolution forecasts with some interesting trends. Figure 9 shows a transition from the precipitation being generated almost entirely from the convection scheme with a 10-minute CCT to predominantly out of the resolved dynamics with a 2-hour CCT.

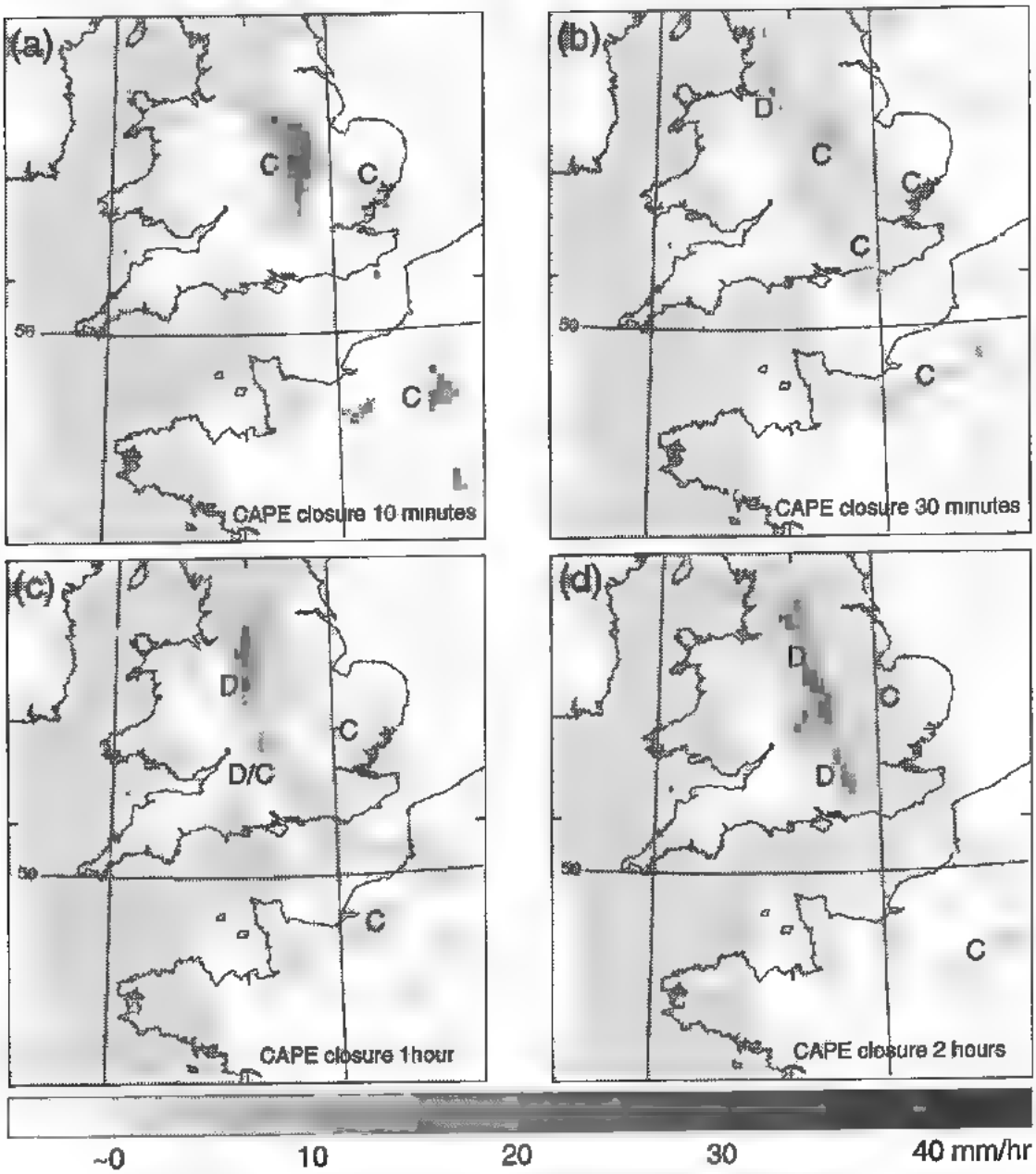

Figure 9. Forecasts of total precipitation rates at 00 UTC 3/7/99 from ND 12km runs with different CAPE closure timescales. ND forecasts started at 15 UTC 2/7/99 after 6 hours data assimilation in the UM at 12km resolution. Rain areas are labelled D when the precipitation comes largely from the resolved dynamics and C when from the convection scheme.

The precipitation rates were highest in the 2 hour CCT run, lower in the 1-hour run and lowest at 30 minutes, then increased again in the 10 minute run. The rain areas over NE France were generated entirely by the convection scheme in all the runs and were therefore most intense in the 10 minute run, but also tended to be located further south (at 00UTC) with shorter CCTs. Over England, the location of the main precipitation region (rates >10mm/hr) varied. The dynamic part propagated eastward more quickly, as well as intensifying and extending southward with longer CCTs; yet it did not get as far east as the convective area in the 10-minute CCT run. The forecast that looked most like the observed radar was the 2-hour CCT run.

6.4 4km resolution forecasts (Figure 10)

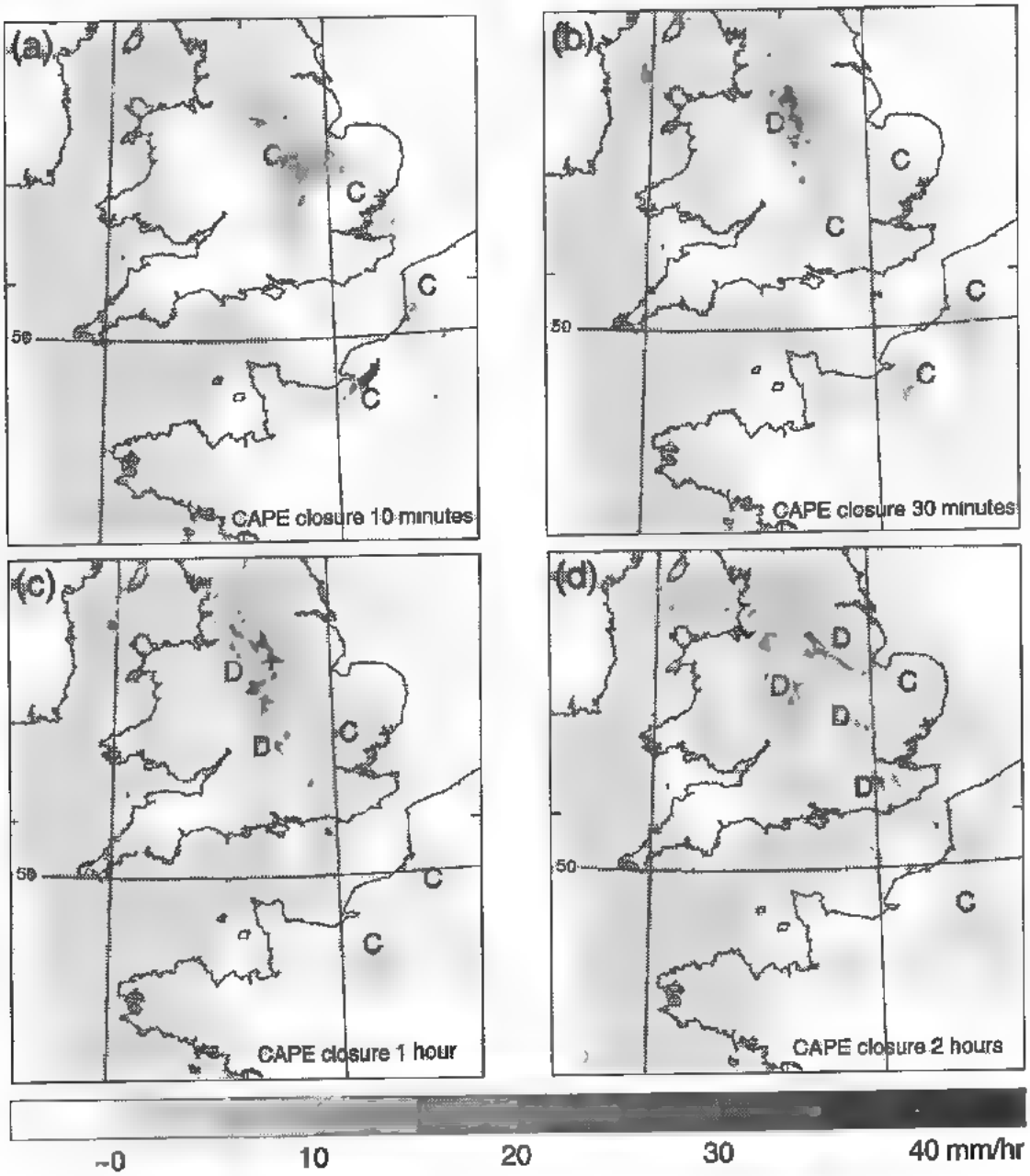

Figure 10. As Figure 9 but for 4km-resolution forecasts.

Most of the trends in the 12km runs were also seen in the 4km runs but more of the precipitation came from the resolved dynamics. The reduced precipitation rates in the

12km run with 30 minute CCT were not evident in the equivalent 4km run because of new development of dynamic rain. This made the 4km/30-minute run look very similar to the 12km/1-hour run in terms of the general rainfall distribution. As at 12km, the convective precipitation regions over NE France intensified and occurred further north (at 00UTC) with shorter CCT, but with systematically heavier and more organised-looking rain. The eastward propagation speed of the resolved dynamic rain also increased at 4km with longer CCTs in the sense that the front edge of the precipitation became further advanced, but the back edge became retarded in the northern part. A squall line developed in the run with a CCT of 2 hours (most northern D in 10d). It is arguable how realistic this is; certainly a squall line developed in reality, however, the scale contraction may be too much and the fragmented nature of the precipitation doesn't compare well with the radar.

6.5 2km resolution forecasts (Figure 11)

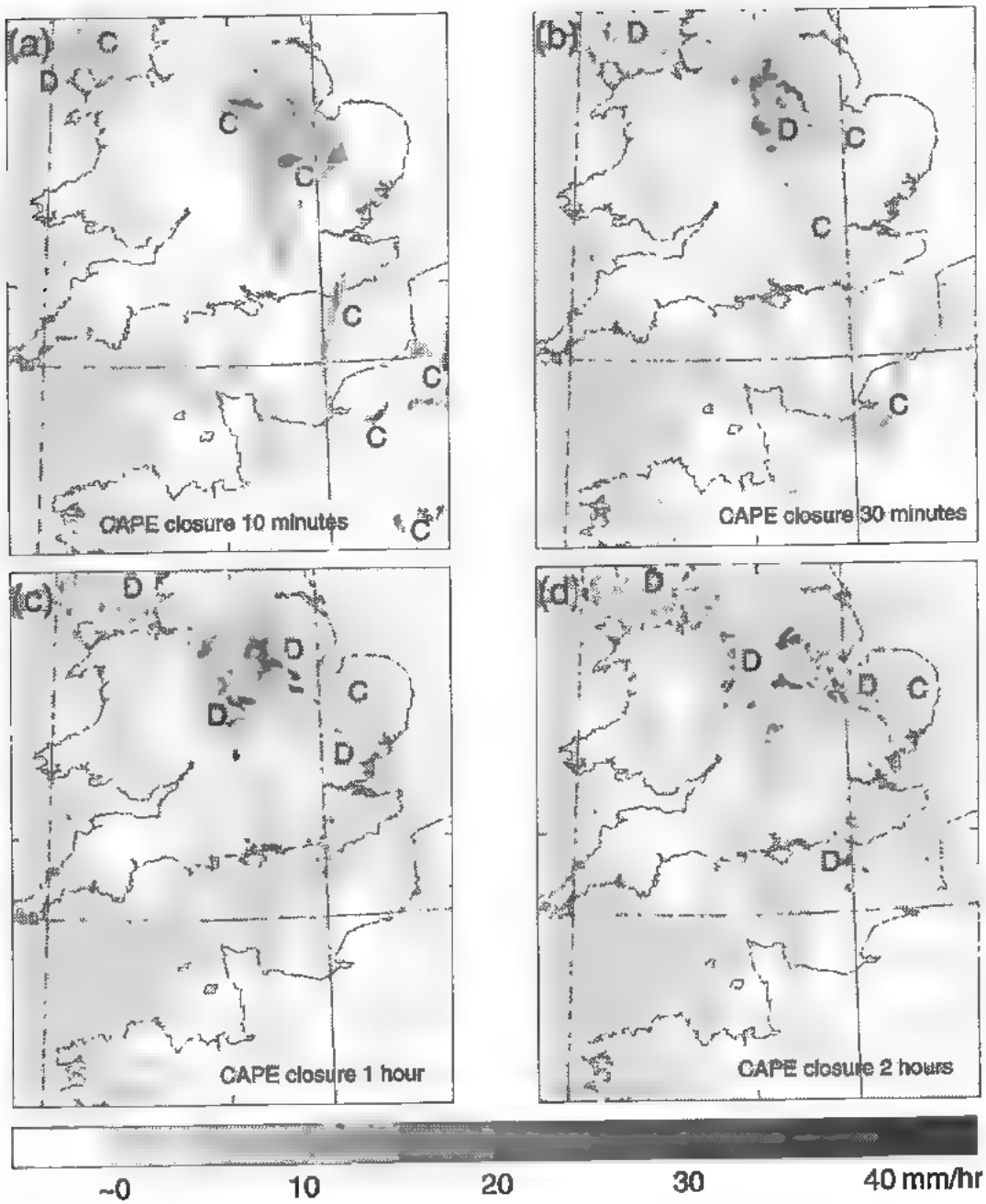

Figure 11. As for Figure 9 but for 2km-resolution forecasts but on the 2km D2 domain.

As with the 12km and 4km runs there was a transition from convective to dynamic precipitation with increasing CCT. At 2km, all significant precipitation came from the resolved dynamics with CCTs of 1 hour or longer. The convective rain over NE France formed distinct bands, was heavy and occurred further south with a CCT of 10 minutes, but had almost vanished when the CCT was increased to 1 hour. The forward edge of the dynamic rain over England advanced further east with increasing CCT especially in the south. The back edge retarded with increasing CCT in the northern part. This was similar to the 4km runs except that at 2km the whole axis of the main rain area twisted much more to become oriented WNW-ESE with a CCT of 2 hours compared to the more NW-SE alignment with 10/30 minute CCT. Squall lines developed in runs with CCTs 30 minutes or longer that looked most coherent and perhaps most realistic in the 2 hour CCT run.

At all resolutions, the runs with a CCT of 10 minutes converged towards a similar rainfall pattern. These runs had smoother precipitation fields than the others with higher CCTs because the rain came mostly from the convection scheme. They therefore fitted best into scenario 1 discussed earlier. The simulations with a long 2-hour CCT developed more fine detail than shorter CCT runs because the rain came mostly from the resolved dynamics. The precipitation patterns were similar in the 2 and 4km runs as scenario 3 was being approached, but varied considerably between 12 and 4km. Other CCTs showed intermediate behaviour.

6.6 The variation in average rainfall rates

Over the time period when the system was in a reasonably steady state (between 21 and 00UTC), we might hope that the average combined dynamic and convective rain rates over some large enough area would be the same whatever the CCT. Figure 12 shows that this is very nearly the case for all the resolutions. The combined average rain rate was almost the same and increased only slightly with longer CCTs at both 2 and 4km, whilst there was a small dip around 60 minutes CCT with 12km resolution. The greater fluctuation in the 4km compared to the 2km runs come from fluctuation in the convective rain and was probably a result of there being fewer gridpoints and more CCTs tested, but may be a real effect.

Dynamic precipitation rates increased and convective precipitation rates decreased with lengthening CCTs as expected from Figures 9,10 and 11. The dynamic rain rate was highest at 2km resolution, slightly less at 4km and markedly less at 12km, which suggests a convergence to some preferred value for each CCT with increasing resolution. The convective precipitation rates were constantly highest in the 12km runs and lowest in the 2km; all decreased at the same rate with lengthening CCTs.

Figure 12 also shows the average rain rates from runs at each of the three resolutions with the convection scheme switched off. All these runs had a higher average rain rate than the equivalent resolution runs with the convection scheme switched on. It is interesting that, from the 'no convection scheme' runs, the 4km had the highest average rain rate and the 12km the lowest. One reason for the 12km run being lowest was that it was slower to develop the storms. Simulations without the convection scheme will be discussed later. A 2km-resolution run was performed with a CCT of 2 weeks. The expectation was that the average rain rate from a run with such a long CCT would approach that from the 2km run without the convection scheme. It was much closer, but still a significant 0.05mm/hr less even though the average rain rate from the convection scheme was nearly zero. More worryingly, despite the low average from the convection scheme with a CCT of 2 weeks, there were some unexpectedly high point convective rain rates in excess of 30mm/hr.

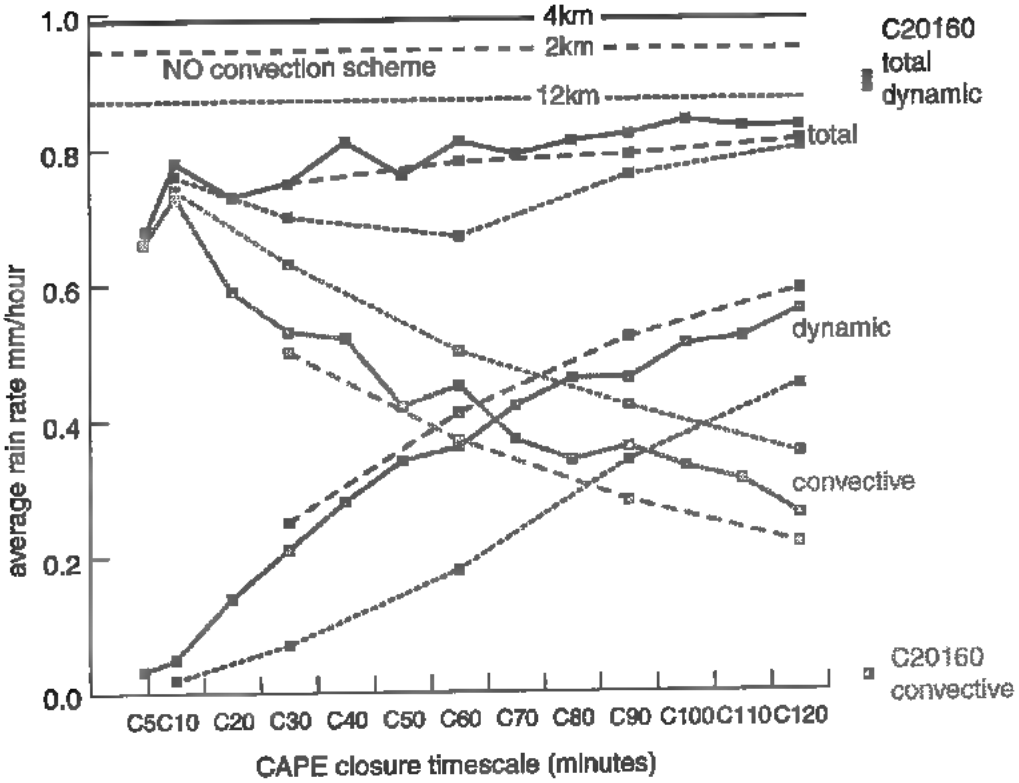

Figure 12. Graph of the average dynamic, convective and total rain rates from ND 9-hour forecasts with CAPE closure timescales of 5 minutes to 2 hours. The average is taken over the 2km domain (see Figure 6) at 10 minute intervals within the period 21 UTC 2/7/99 to 00 UTC 3/7/99. Dotted lines are the 12km runs; continuous lines are the 4km runs and dashed lines the 2km runs. The points labelled C20160 refer to a 4km forecast with a CAPE closure timescale of 2 weeks. The lines at the top show the average rain rate from a 12km run (short dashes), 4km run (continuous) and 2km run (longer dashes) with the convection scheme switched OFF.

6.7 The variation in the peak rain rates

In addition to examining the average precipitation rates and the rainfall distribution it is worth looking at changes in the peak precipitation rates with different CCTs for strong convective events. With a progression to higher resolutions (5km or better) the model should be able to predict the rainfall intensities that might actually be observed by rain gauges or radar (at similar resolution), thus adding an extra dimension to the information that can be extracted from a forecast.

First, a look at 12 km resolution from the first graph in Figure 13. The variation in peak rain rates varied in the same way with different CCTs in both the UM and ND. Both had peak dynamic rates that increased and peak convective rates that decreased with lengthening CCT and both had a minimum in the total rate at around 30 minutes CCT. The combined total peak rain rate, in both models, with CCTs greater than 90 minutes was more than twice that with the CCT of 30 minutes. The ND had consistently lower peak rates than the UM. The simulations with the longer CCTs produced precipitation that was too intense compared with that observed from the radar, yet despite this, it was the 2 hour CCT run that developed the most realistic looking precipitation pattern (Figure 9). It should be pointed out that the graphs in Figure 13 are constructed from only a few points and each point represents only a small amount of data. Sampling at more frequent time intervals and running with more CCTs would be better, but limited time and disk space has prevented this so far.

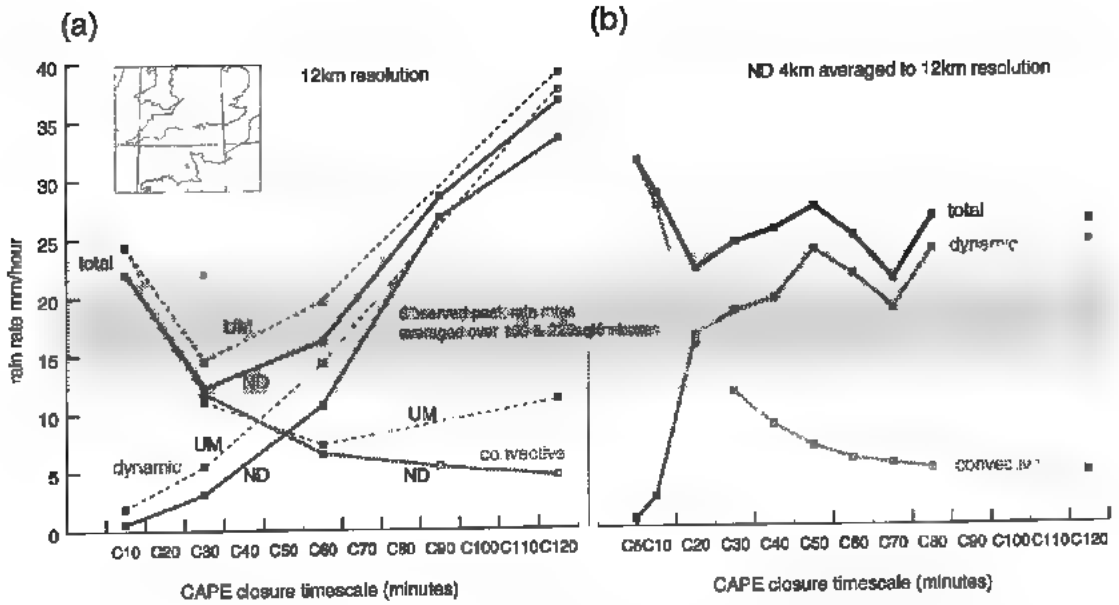

Figure 13. Graphs of peak dynamic, convective and total rain rates for different CAPE closure timescales over the area shown. The total peak rate was found by adding the dynamic and convective at each gridpoint and finding the highest, not by adding together the highest dynamic and convective found within the area. The shading shows the observed estimate of peak rainfall rates at 10-15km resolution from the 5km resolution network radar. (a) 12km resolution. The average of the peak rainfall rates taken from 21 and 00UTC. The continuous line connects the ND 12km (45 level) runs and the dashed line the UM 12km (38 level) runs. The isolated point at 30 minutes CAPE closure is for the UM run shown in Figure 8a. (b) 4km resolution. The average of the peak rainfall rates at 22, 23 and 00 UTC from the ND 4km runs averaged to 12km.

The isolated point is from a UM run that had a climatological soil moisture ancillary field rather than the updated one used by the other runs. It is included because the ND runs used this climatological field; hence why this UM run was shown as a comparison with the ND in Figure 8(a).

The results from the 4km runs are shown in Figure 13(b). The peak rain rates have been averaged to 12km resolution for a direct comparison with Figure 13(a). At 4km resolution the peak rates showed less variability than at 12km and the dip at 20-30 minute CCT was much less evident. The peak rain rates were much more realistic with the longer CCTs than at 12km. In this case there was benefit from extracting lower-resolution information from the high resolution simulations. The dip in the run with a CCT of 70 minutes associated with a dip in the dynamic peak rate may be evidence of a real effect, but is probably due to insufficient sampling frequency.

6.8 Key results from varying the CAPE Closure Timescale (CCT)

- The distribution of rainfall and the peak rainfall rates were very sensitive to changes in the CCT in the UM and ND at all the resolutions tested.
- The average precipitation rates remained nearly constant, only slowly increasing with longer CCTs.
- The 4km resolution ND run with 30 minutes CCT was most comparable in terms of precipitation distribution to the 12km ND run with 1 hour CCT.

- The average precipitation rate with the convection scheme switched on was always less than with the convection scheme switched off, even with a CCT of 2 weeks.
- The front edge of the dynamic precipitation propagated forward more quickly with longer CCTs at all the resolutions.
- The 2km runs developed squall lines when the CCT was 30 minutes or longer, this only happened at 4km with a 2 hour CCT and not at all in the 12km runs.
- The 12km ND looked most realistic compared to the radar with a CCT of 2 hours, but peak rain rates were too high.
- It is unclear what runs were the most realistic at 4km or 2km resolution. An assessment of longer CCTs and the runs with no convection scheme (Section 9) should be made.
- Unrealistic regions/bands of convective precipitation occurred over NE France with lower CCTs at all the ND resolutions (and in the 12km UM). These were most dramatic at 2km with a CCT of 10 minutes, but with a 1-hour CCT they were most noticeable in the 4km run.
- If the ND is to be run at high resolution and the current convection scheme is to be used and switched on, it is essential that the optimal CCT is found because it can have a big impact on the precipitation forecast. Further studies should be done.
- With a short CCT of 10-minutes the solutions at all three resolutions appeared to be determined by the scales of the convection scheme and fit into scenario 1 discussed at the start of the section.

7. Unrealistic convective rainbands

One of the findings from the previous section was that bands of convective precipitation, which were not observed in reality, developed over NE France in all the ND runs with shorter CCTs (30 minutes – 1 hour or less). In fact, they occurred not only at 00UTC over NE France as seen in Figures 9-11, but throughout the forecast period ahead of and in the vicinity of the main rain area along the middle-level frontal zone.

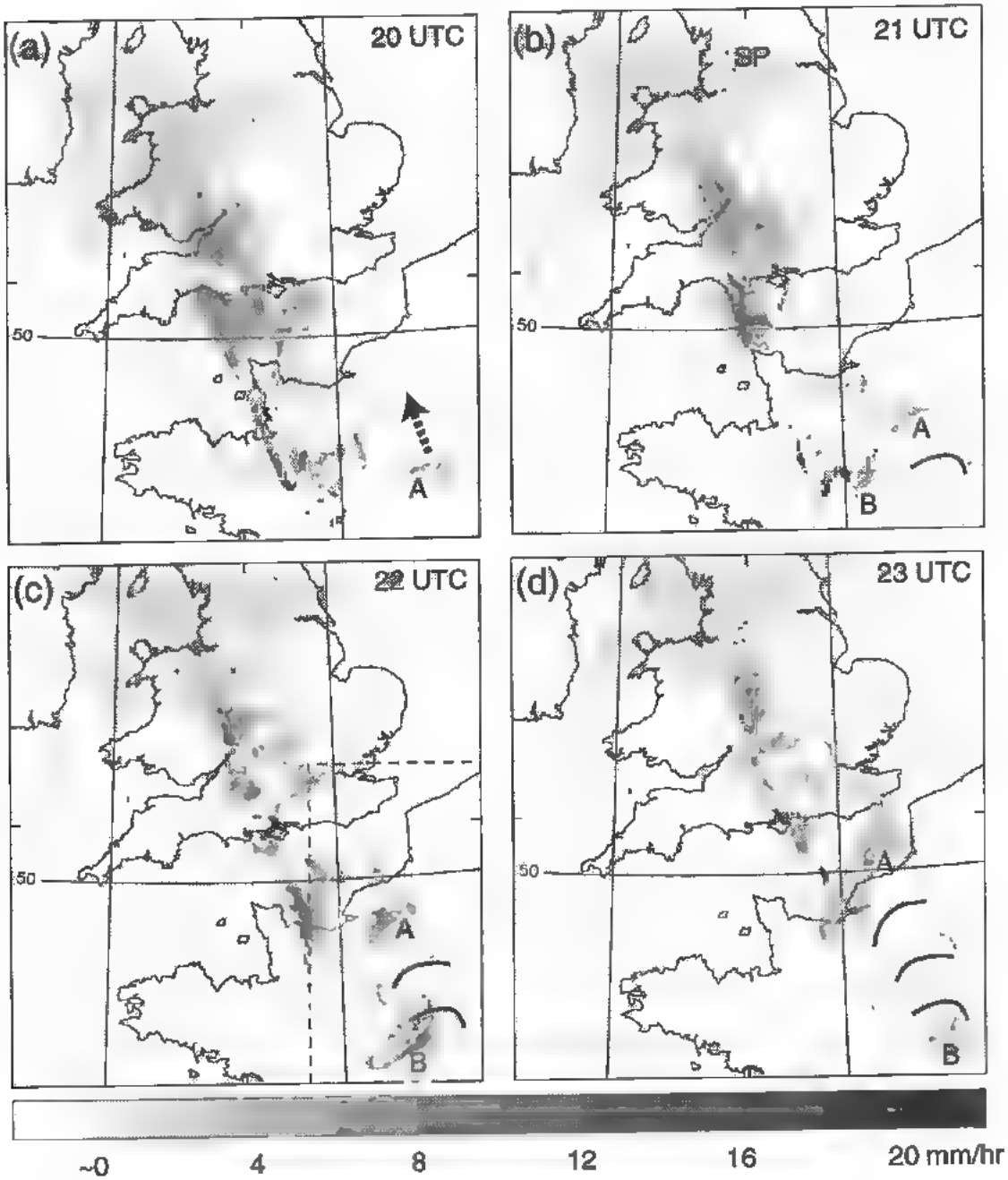

Figure 14. Convective rain rates only at 20,21,22 and 23 UTC 2/7/99 from the ND 4km forecast starting at 15UTC with a 30 minute CTT (total rain rates at 00 UTC 3/7/99 from this run are shown in Figure 9b). The letters A and B label convective rain areas that can be easily tracked. The dashed arrow in (a) shows the direction of movement of area A. The lines in (b), (c) and (d) show the axis of the previous positions of area A. SP in (b) indicates a region of 'speckled' convection (also seen in the other frames).

Animation sequences revealed that these convective rainbands propagated rapidly, spreading outwards like ripples from stones thrown into a pond. They propagated mostly in a NW-SE direction along the frontal zone and gave the impression of looking like gravity waves. The impact on the forecast was not only to produce convective rain where there shouldn't have been any, but also to retard and weaken the main dynamic precipitation area. In addition, dynamic precipitation was triggered in places where the convective rainbands collided with each other and where the convective rainbands interacted with the middle-level frontal zone.

7.1 Description of the rainbands in a 4km run with a 30-minute CCT

The propagation and spreading out of bands of convective rain in the ND 4km run are shown in Figure 14. The precipitation rates are not insignificant with intensities of more than 10mm/hr. Further discussion will concentrate on the band labelled 'A'. This band propagated rapidly northward and was eventually associated with new triggering of resolved dynamic precipitation over eastern England after 01 UTC 3/7/99 (not shown).

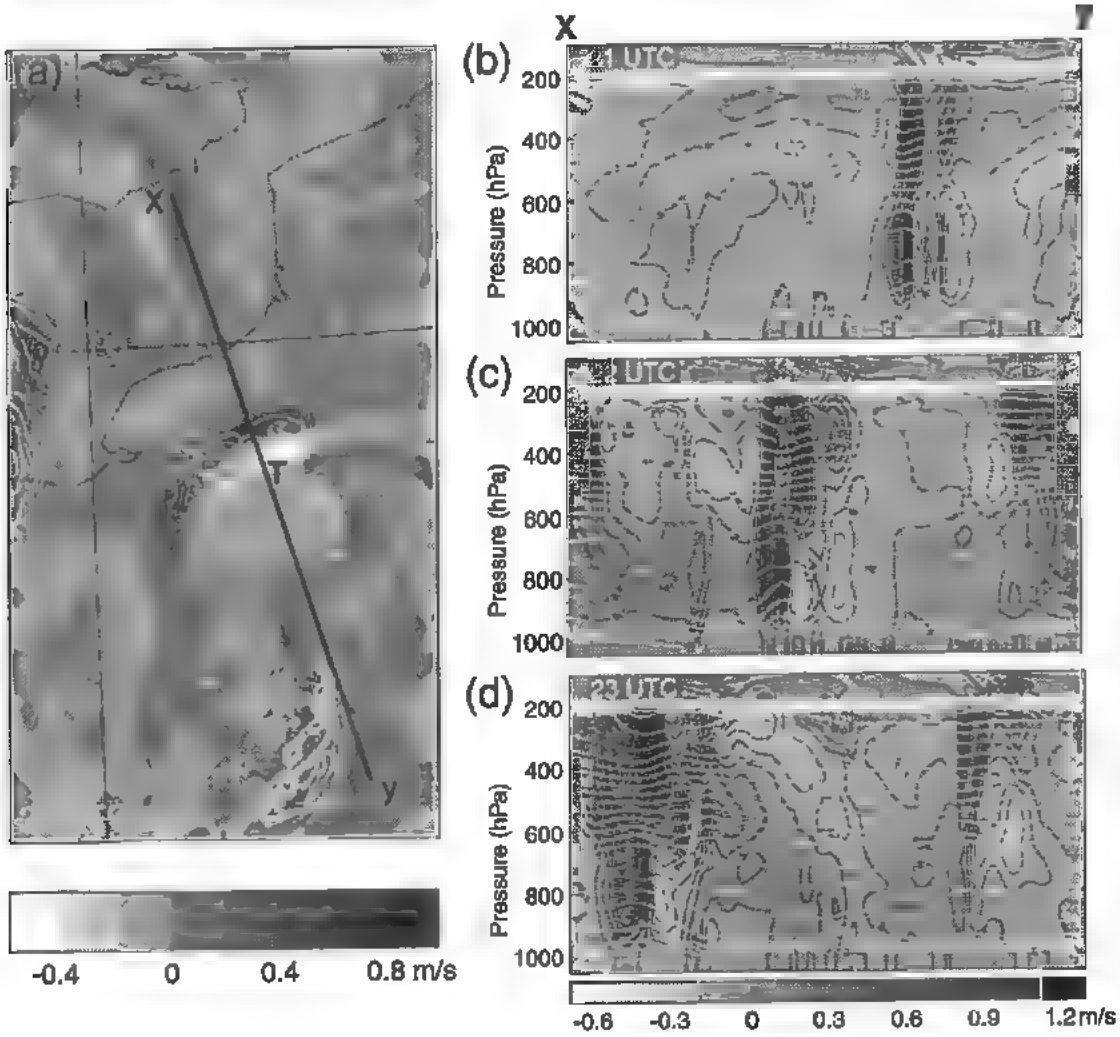

Figure 15. Output from ND 4km resolution forecast starting at 15UTC with a 30-minute CCT. (a) 22UTC 2/7/99. Area is shown by the dashed box in Figure 14c. Shading is vertical velocity at 800 hPa. White contours show the convective precipitation rate at 4mm/hr intervals. The line XY marks the location of the cross-section shown in b, c and d. The letter T marks the position of the tephigram shown in Figure 16a. (b), (c) and (d) Cross-section XY at 21, 22 and 23 UTC 2/7/99. Shading shows vertical velocity. White contours show potential temperature.

A closer look at the rainband in Figure 15a reveals that the convection scheme precipitation was coincident with resolved scale vertical velocities at 800hPa of up to 1m/s. The cross-sections in Figure 15 show a maximum vertical-velocity core around 800 hPa and another at around 400 hPa; both propagated north-northwest, the lower one at 27m/s and the upper one slightly more slowly. The lower vertical velocity core was part of an ascent-descent dipole with a region of descent behind the ascent (to the south). Between the ascending and descending parts there was a cold pool, shown by the bending upwards of the isentropic surfaces. Along the cross section at 900hPa the cold pool was some 2°C colder than its surroundings.

7.2 A probable mechanism

It would appear that there was some interaction between the convection scheme and the dynamics. The tephigram in Figure 16 shows two profiles; one from the 4km 30-minute CCT run (solid lines) at a time and place where convective rainband A has just passed through; the other at the same time and location (dashed lines) from a 4km run with the convection scheme switched off. Both profiles show that convection would be possible from around 750hPa if there was any localised lifting and that any convection that did occur could reach the tropopause (230hPa) and have a large amount of CAPE. The differences between the two profiles show that the convection scheme has acted to dry the model atmosphere between 870 and 730hPa and cool it by around 2°C below 800hPa.

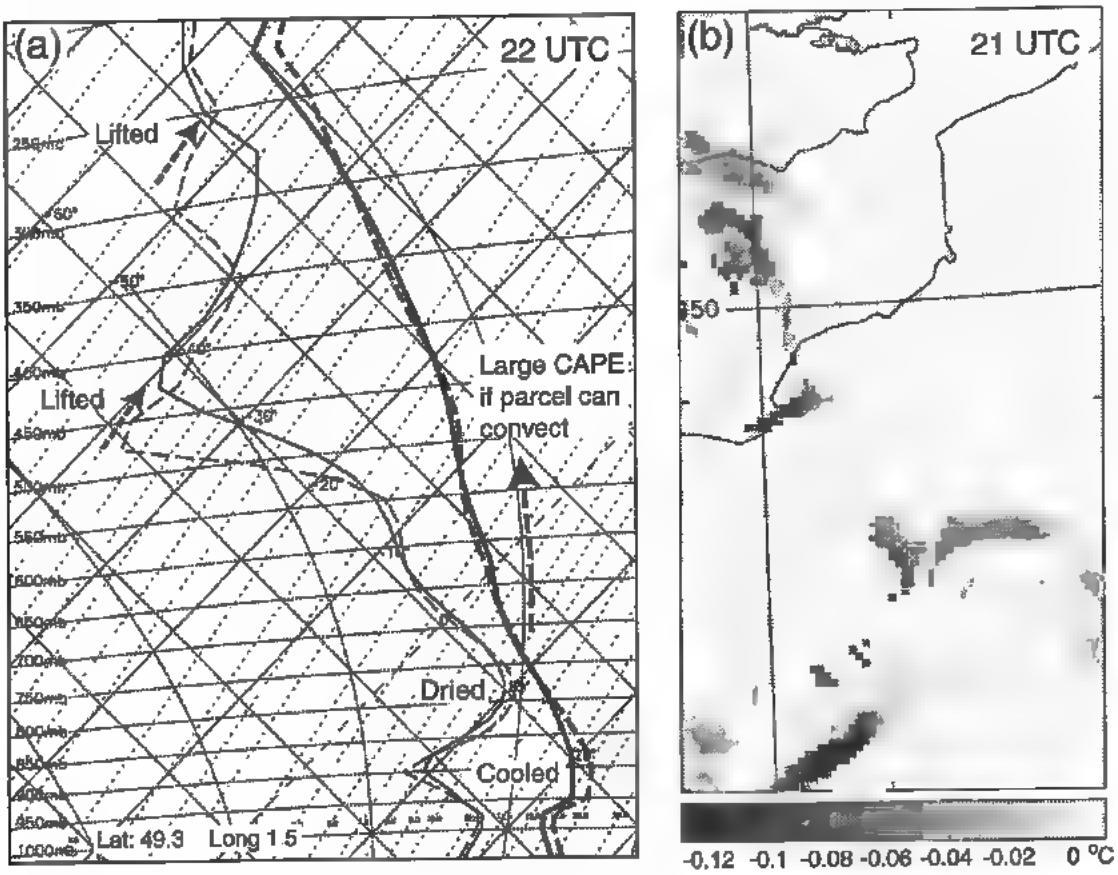

Figure 16. (a) Tephigram at 22 UTC 2/7/99 at the position marked with a letter T in Figure 15a. The profile shown by the continuous lines is from the 4km run with a 30-minute CCT; the profile shown by the dashed lines is from a 4km run with the convection scheme switched off. (b) Temperature increments from the convection scheme at 21 UTC, (2-minute timestep) from the 30-minute CCT run.

The temperature increments from the convection scheme at model level 7 (~920 hPa) after a timestep are shown in Figure 16b. Model-level 7 was being cooled by convective band A at a rate of up to 0.1°C every timestep. This would amount to a cooling at a gridpoint of up to 1.2°C as the convective band passed through, assuming a band width of 10 gridpoints (typical for 22UTC), velocity of 27m/s and timestep of 2 minutes. The convection scheme therefore seems to be crucial to the formation of the cold pool.

Further evidence for the vertical motion shown in the Figure-15 cross-section sequence can be extracted from the tephigrams. The shape of the dew-point profiles from both runs look similar except that the one from the run with the convection scheme operating appears to be elevated by 50 hPa compared to the other. This is indicative of 50hPa ascent, which can be converted into a vertical velocity of 0.6-0.8m/s over 12 minutes if it is assumed that the ascent took place over 5 gridpoints. Above 800hPa, the two dry-bulb profiles are almost identical due to the cooling associated with the ascent being offset by the warming from the convection.

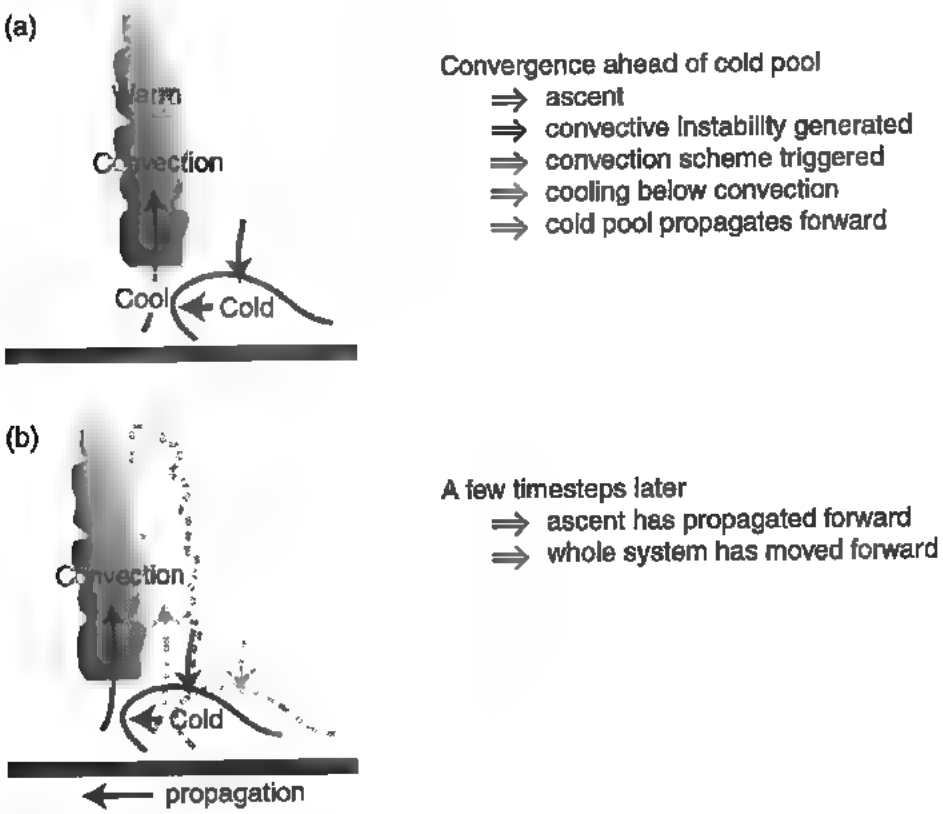

Figure 17. Schematic of the probable mechanism associated with the convective bands.

A likely mechanism is drawn schematically in Figure 17. The convection scheme was firstly triggered at gridpoints where there was sufficient moisture and local ascent at around 750hPa to make the profile conditionally unstable. The convection scheme cooled the profile below the convective plume. If convection continued, then further cooling generated a low-level cold pool and the dynamics responded with a region of convergence and ascent ahead of the cold pool as a local frontal zone or density current structure developed. The maximum cooling was not at the lowest levels; therefore the lower levels would become more unstable and overturning in the boundary layer may have helped to re-trigger the convection in the early stages. As the density current became established the ascent ahead of the cold pool acted to destabilise the profile and trigger further convection which in turn cooled the region ahead of the cold pool and propagated

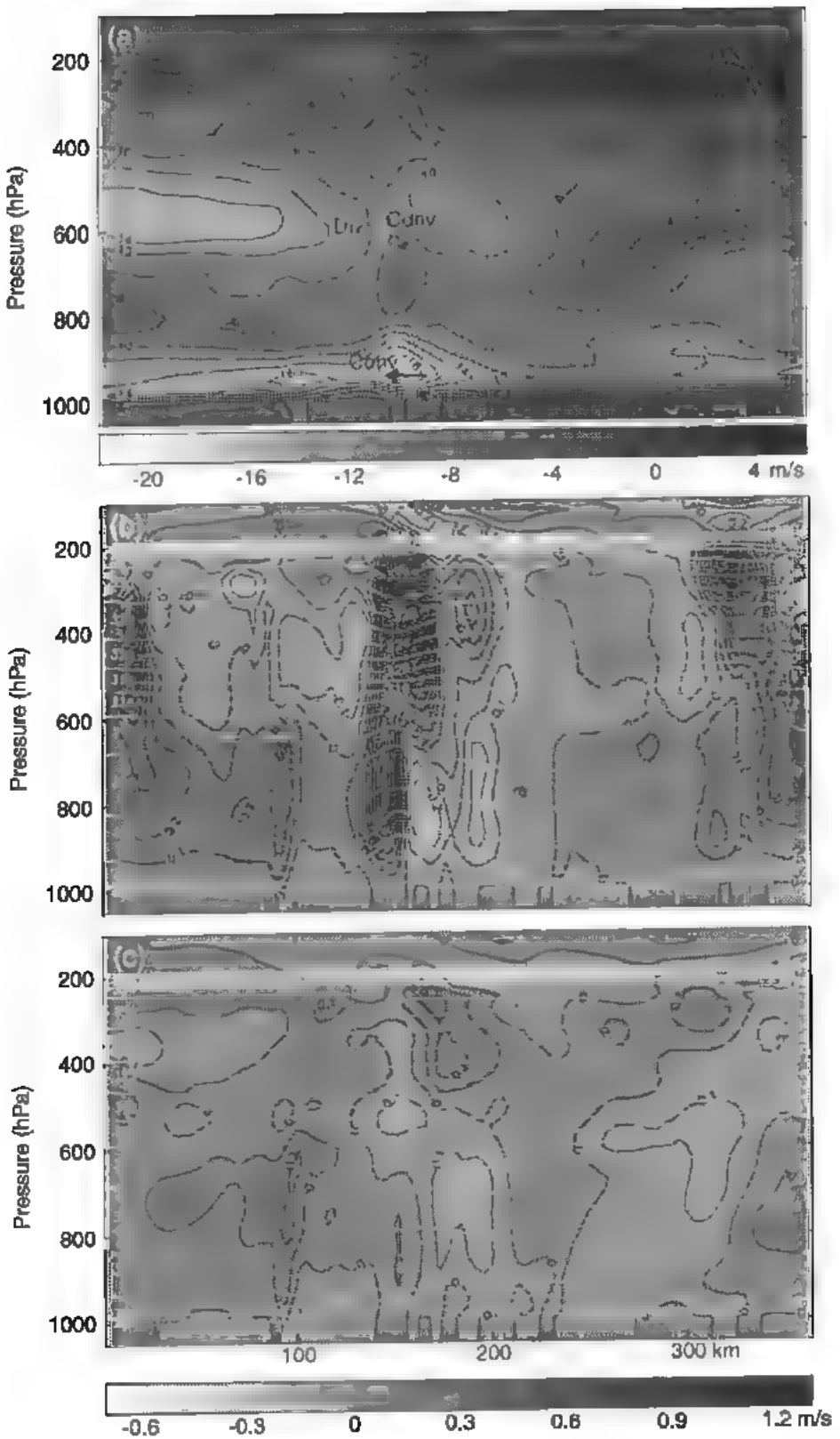

Figure 18. Cross-sections along XY in Figure 15a, all at 22UTC 2/7/99. (a) ND 4km resolution forecast from 15UTC with a 30-minute CCT. Shading is wind speed along the section. White contours are vertical velocity at 0.5 and 1m/s. Black arrow shows the strongest along-section flow. Conv and Div refer to regions of convergence and divergence in the 2 dimensions of the section. (b) Same ND run as (a). Shading is vertical velocity; white contours are potential temperature (enlargement of Figure 15c). (c) Same shading and contouring as (b) for a run with a CCT of 30 minutes up to 21 UTC then with the convection scheme switched off.

forward the cold pool and ascent region. A self-maintaining system developed as long as the surrounding environment had sufficient unrealised potential instability. The cross-sections in Figure 18a&b show how the density current flow, vertical velocity and cold pool associated with convection band A fitted together at 22UTC – they form the basis of the schematic Figure 17.

The upper region of ascent probably resulted from the combination of a region of convergence at the top of the lower region of ascent, heating from the convection scheme and a strong along isentropic flow relative to the propagating convection.

7.3 The effect of switching off the convection scheme after 6 hours

If the convection scheme was so important in the development and maintenance of the gravity current type phenomena just described, then switching off the convection scheme part way through a run should have had a dramatic effect. An experiment was performed in which the 4km resolution run with a 30-minute CCT was run for 6 hours up to 21UTC and then run for a further 3 hours with the convection scheme switched off. The output from this run after 21 UTC was compared with that from the 4km run with a 30-minute CCT throughout. The difference between the two runs at 22UTC can be seen by looking at the cross-sections in Figure 18b and c. In the run with the convection scheme turned off the cold pool and ascent regions have almost completely vanished; this after only 1 hour. In fact, much of the feature was destroyed after only 20 minutes. This is further evidence that the convection scheme was essential for the maintenance of the structure in the dynamics. If it were a pure gravity wave, the expectation is that it would have continued to persist much longer.

7.4 Summary of this section

- Propagating bands of convective precipitation developed in all the runs in which the CCT was sufficiently short (30 minutes or less at 2 & 12 km resolution, 1 hour or less at 4km resolution)
- The bands were coincident with resolved vertical velocities of over 1m/s.
- Phenomena like this were not observed in reality.
- Propagation speed were fast, 20-30m/s.
- They acted to retard and weaken the precipitation that came from the resolved dynamics as well as sometimes causing new dynamic precipitation to be initiated.
- The probable mechanism was a coupling between the convection scheme and the dynamics. Temperature increments from the convection scheme lead to vertical motion in the dynamics which in turn triggered the convection scheme.
- This behaviour in high-resolution models is undesirable. It is not known how often this could be a problem. Further case studies are required.
- The CAPE closure timescale in the convection scheme is crucial. If the current convection scheme is to be used for high resolution forecasting, then a safe lower value for the CAPE closure timescale should be known.
- Further investigation to clarify the mechanism is required.

8. Changing the timestep at 4km resolution

The 4km resolution simulation with a 30-minute CCT was re-run several times with a different timestep, primarily to see if the propagation speed of the convective rainbands would vary, but also to look at the general impact on the forecast. It was thought that the propagation speed of the convective rainbands described in the previous section might be sensitive to the timestep. The reasoning was that since the rainbands moved at close to one gridlength per timestep there might have been a discrete propagation from gridpoint to gridpoint. In which case, a halving of the timestep might simply double the propagation speed. However, density current propagation is dependant on ΔT and ΔT depends on CCT not Δt.

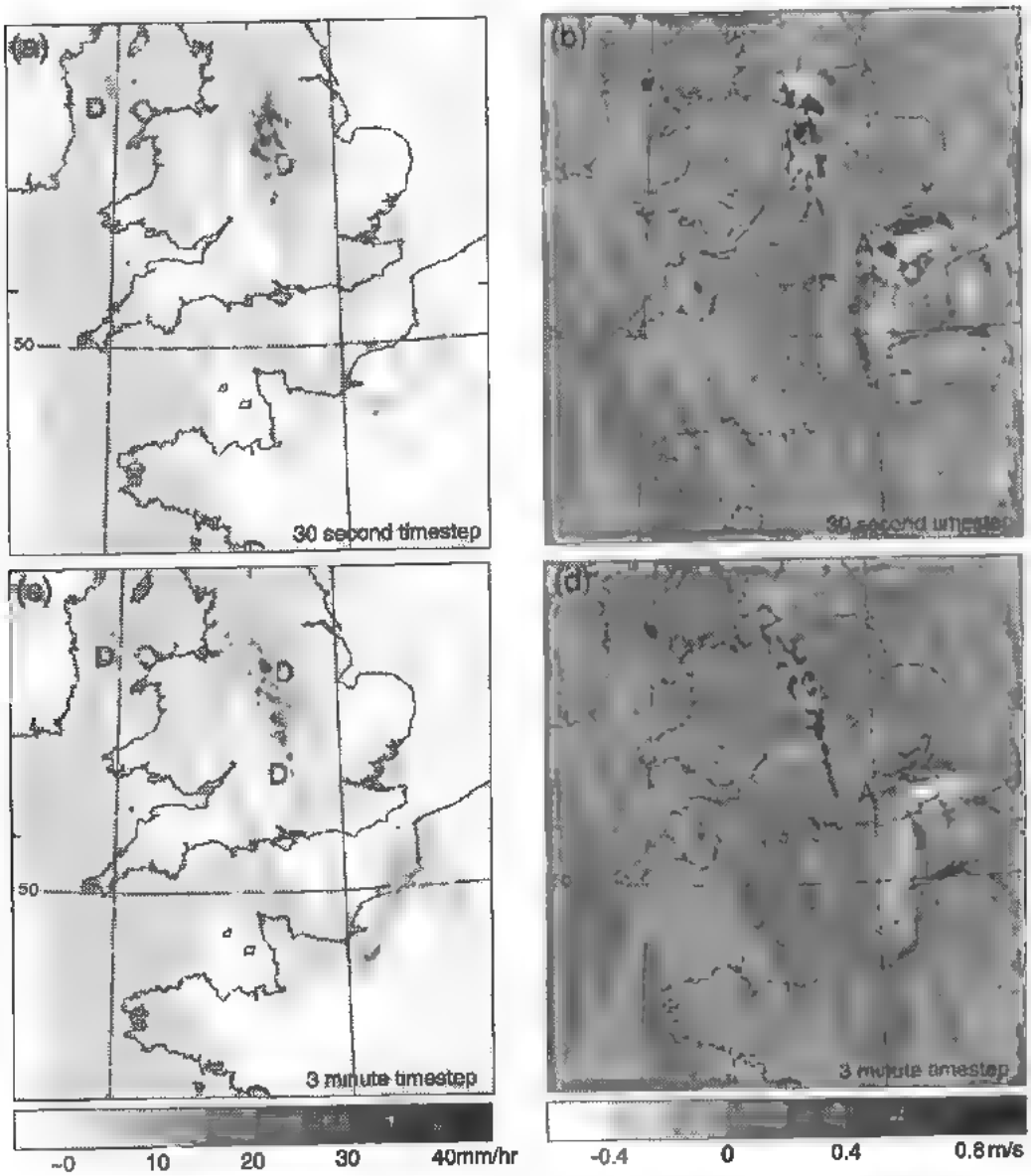

Figure 19. Output from ND 4km resolution runs with different timesteps starting at 15UTC 2/7/99 valid at 00UTC 3/7/99. 30-minute CCT. (a) Precipitation rates from a 30-second timestep run; the letter D refers to mostly dynamic precipitation. (b) Vertical velocity at 800hPa from the 30-second timestep run; the letter A shows the location of band A described in the previous section. (c) Precipitation rates from a 3-minute timestep run. (d) Vertical velocity at 800hPa from the 3-minute timestep run.

Changing the length of the timestep had no effect at all on the propagation speeds. The region of ascent associated with convective rainband A (see previous section) is labelled A on Figure 19c & d for the 30-second and 3-minute timestep runs and there is practically no difference in position. However, the bands were not identical in the two runs; they were somewhat more coherent in the 3-minute timestep run and there were differences in evolution and intensity. Significant differences were seen in the distribution and intensity of the precipitation that came from the resolved dynamics as shown in Figure 19a & c. With longer timesteps the resolved precipitation area became more linear, was generally less intense and extended further south. The reason for this is not clear without further investigation.

The vertical CFL numbers for the most intense storm cells have been calculated (Table 2). The CFL number is the number of vertical levels or horizontal gridsquares the back trajectory of an airparcel travels through in a single timestep. If this number is greater than 1 then accuracy is reduced and this was likely to be the case with the large vertical velocities associated with a simulation of deep convection. The expectation was that the CFL numbers would be largest in the runs with the longest timestep. This was not the case because the highest vertical velocities decreased with increasing timestep. The largest CFL numbers did exceed 1 (for the 1-3 minutes timestep runs) but rarely exceeded 2 even with a 3-minute timestep.

Timestep	Maximum W	Average maximum W	Maximum CFL number
1 minute	10.0 m/s	8.3 m/s	1.3 - 1.6
2 minutes	7.3 m/s	6.8 m/s	2.2 - 2.4
3 minutes	4.7m/s	3.4 m/s	1.7 - 2.3

Table 2. From 21,22,23 & 00 UTC vertical velocity fields. The maximum is the highest found. The average maximum is the average of the highest at each time.

Figure 20 reveals that the average precipitation rate from the resolved dynamics, over the whole domain, decreased with lengthening timestep and that the average precipitation rate from the convection scheme increased with lengthening timestep. The total average precipitation rate remained roughly constant. Intuitively, it seems reasonable that the dynamic precipitation should increase with shorter timesteps because this would allow greater organisation of small-scale features to intensify the rain area. It is interesting that the change in the average dynamic rain rate was almost exactly equal and opposite to the change in the average convective rain rate. This implies that the same amount of instability was being consumed even when the ratio of resolved to parametrized precipitation was altered.

Although the 3-minute timestep run did not fail and the precipitation looked reasonable, the potential vorticity field broke down into a grid-scale checkerboard pattern (not shown).

The run with a 4-minute timestep failed after running for nearly two and a half hours. The 800hPa vertical velocity field a few minutes before failure is shown in Figure 21. This kind of checkerboard pattern has been observed before (P A Clark, private communication). On those occasions as here the problem came from the diffusion and shouldn't have occurred. A diffusion coefficient was set which should have theoretically remained stable and decayed instability. It may be that there was a complex interaction between the diffusion and the semi-lagrangian dynamics, or perhaps an error in the code. This issue does require further investigation because even though the intention is to run the ND with very little diffusion, this may not be possible at very high resolution.

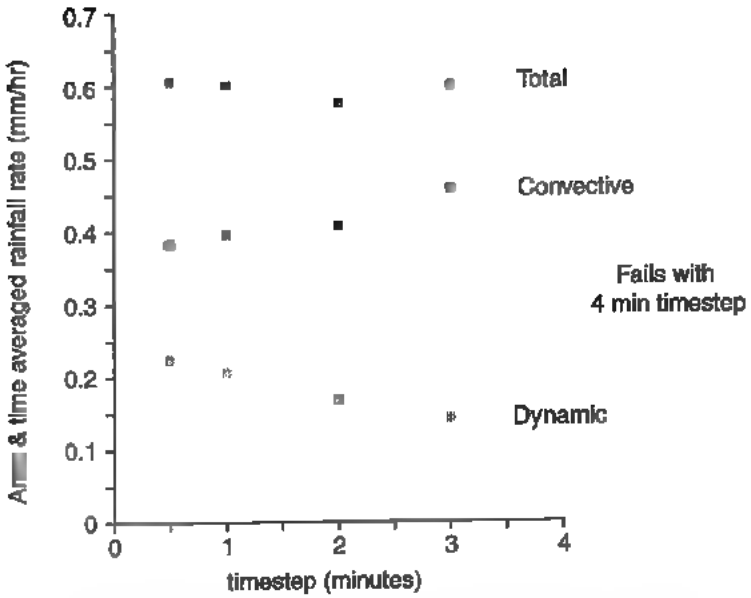

Figure 20. A graph of the average dynamic, convective and total rainfall rates against length of timestep for ND runs starting at 15UTC 2/7/99. The precipitation was averaged over the 4km domain D4 and over a 3-hour period from 21UTC 2/7/99 to 00UTC 3/7/99. Sampling took place every 10 minutes for the 0.5, 1 and 2 minute timestep runs and every 9 minutes for the 3-minute timestep run.

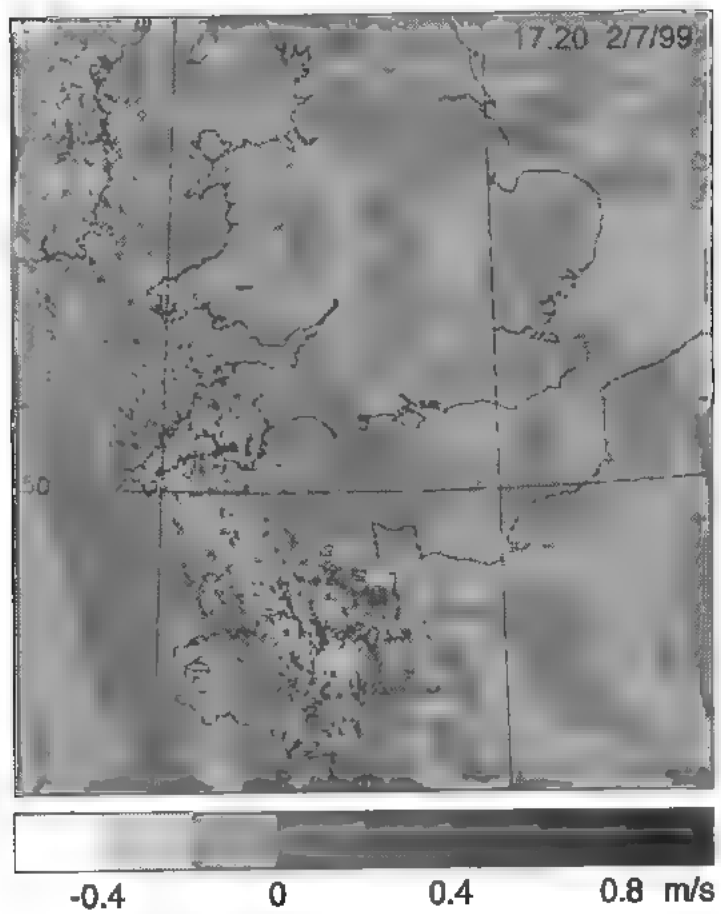

Figure 21. Checkerboard noise in the 800hPa vertical velocity at 17.20 from a 4km ND run starting at 15UTC 2/7/99 with a 4-minute timestep. The run failed shortly after this time.

9. Running without the convection scheme

As the resolution of numerical forecast models is continually improved, the issue of deciding at what resolution it is possible to represent convective processes without the need for a convection scheme has arisen. The benefit of running without a convection scheme at high resolution is that it is likely to give more meteorologically realistic forecasts and provide extra information at small scales which can be useful after averaging to larger scales. The downside is that the location and intensity of individual storm cells can't be believed because they may be stochastic in nature. Simulations with slightly different initial conditions will develop storm cells in different locations within the envelope of convective activity. For a high resolution run without a convection scheme to produce better forecast skill without averaging, the initial fields (large and grid scale) must be sufficiently accurate – a data assimilation problem. Nevertheless, running without a convection scheme might still be the best choice, particularly for nowcasting and because currently available convection schemes may not behave well at high resolution.

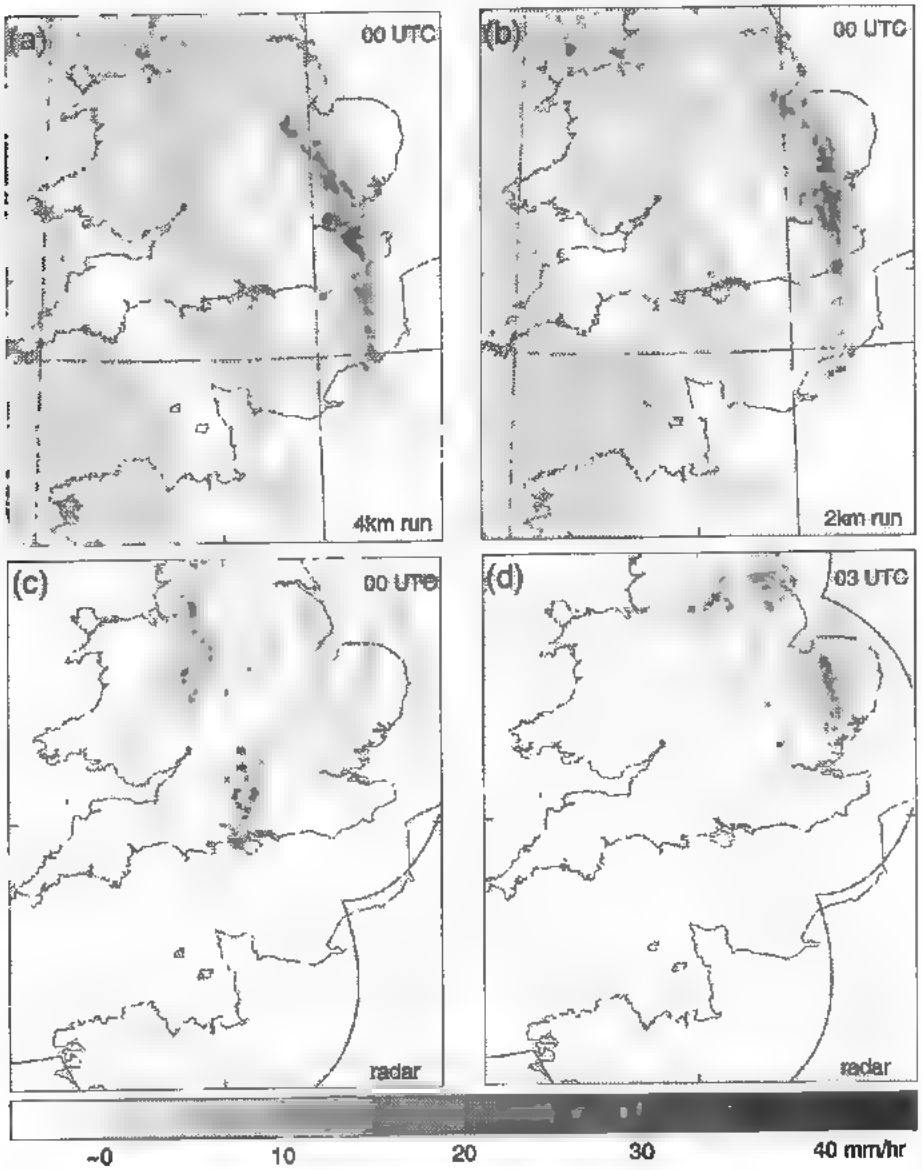

Figure 22. (a) and (b) The precipitation rates at 00UTC 3/7/99 from 4km and 2km resolution ND runs starting at 15UTC 2/7/99 with the convection scheme switched off. The rain rates have been averaged to 5km resolution for comparison with the radar. (c) and (d) The network radar pictures for 00 and 03UTC 3/7/99.

Organised convective systems, like the one being discussed in this report, are likely to be the easiest type of convection to represent explicitly. Weisman et al, from a study of quasi-three-dimensional squall line simulations, concluded that a resolution of 4km is sufficient to reproduce nearly all of the structure produced by a 1km-resolution simulation.

The ND has been run at 12, 4 and 2km resolution from 15UTC 2/7/99 with the convection scheme switched off. Figure 22 shows the precipitation at 00UTC 3/7/99 from the 4 and 2km runs (averaged to 5km) compared with the radar. The precipitation patterns were very similar, but the rain had advanced further east in the 2km simulation. Both runs had propagated the rain further east than their equivalent runs with the convection scheme switched on (all CCTs) and produced a more 2-dimensional squall line structure.

It would appear that these forecasts verify worse against the 00UTC radar picture in terms of the position of the rainfall than the runs using the convection scheme. However, care must be taken when comparing against observations. The initial state used for the high-resolution simulations was taken from a 12km resolution UM mesoscale analysis that had the dry intrusion and mid-level frontal zone in a more advanced position than the satellite imagery indicated (Figure 5). It should therefore be expected that the rainband in the model simulations would be further east than observed if the convection was driven by the larger scale dynamics. The verification of the two ND model runs against the 03UTC radar picture is very good in terms of the structure of the precipitation; a squall line structure was observed as well as simulated and the rainfall intensities were similar - though higher in the model runs.

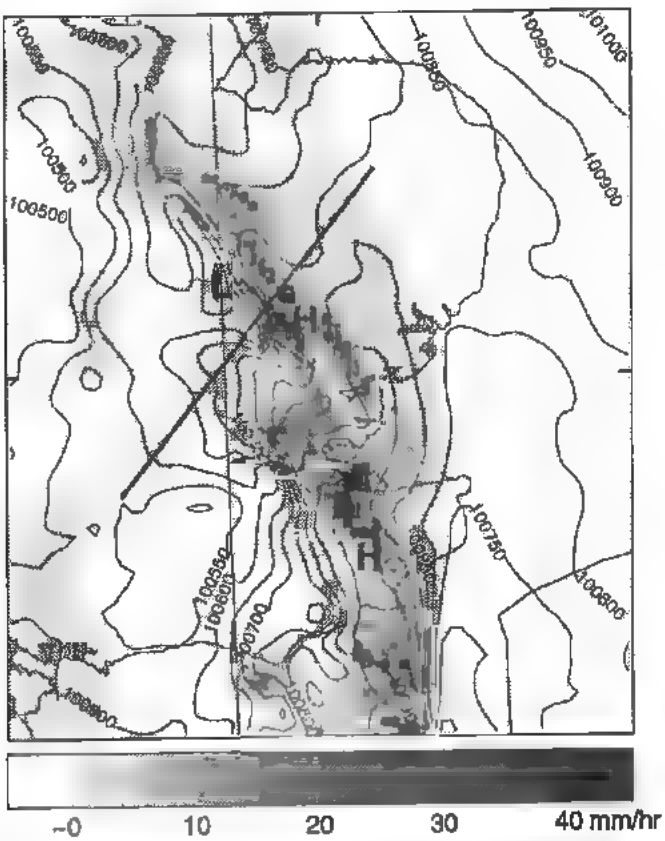

Figure 23. Squall line at 00UTC 3/7/99 from the ND 12 hour forecast at 4km resolution with no convection scheme. Shading is precipitation rate. Contours show sea-level pressure at 0.5hPa intervals (labelled in Pa). The letters H and L indicate meso-high and low pressure regions. The black line shows the location of the cross-section in Figure 24.

Figures 23 and 24 have been included to show that the 4km-resolution simulation without the convection scheme produced a realistic looking squall line. The cross-section is through a nearly 2-dimensional part of the line of storms and shows the ascent of over 5m/s. Relative to the movement of the squall line, the dry air behind at mid-levels was approaching at up to 12m/s and the lower-level inflow was feeding in at around 8m/s. The descent behind the updraught was greater than 2m/s. The CFL number for ascent of 5m/s and a timestep of 2 minutes is around 1.7.

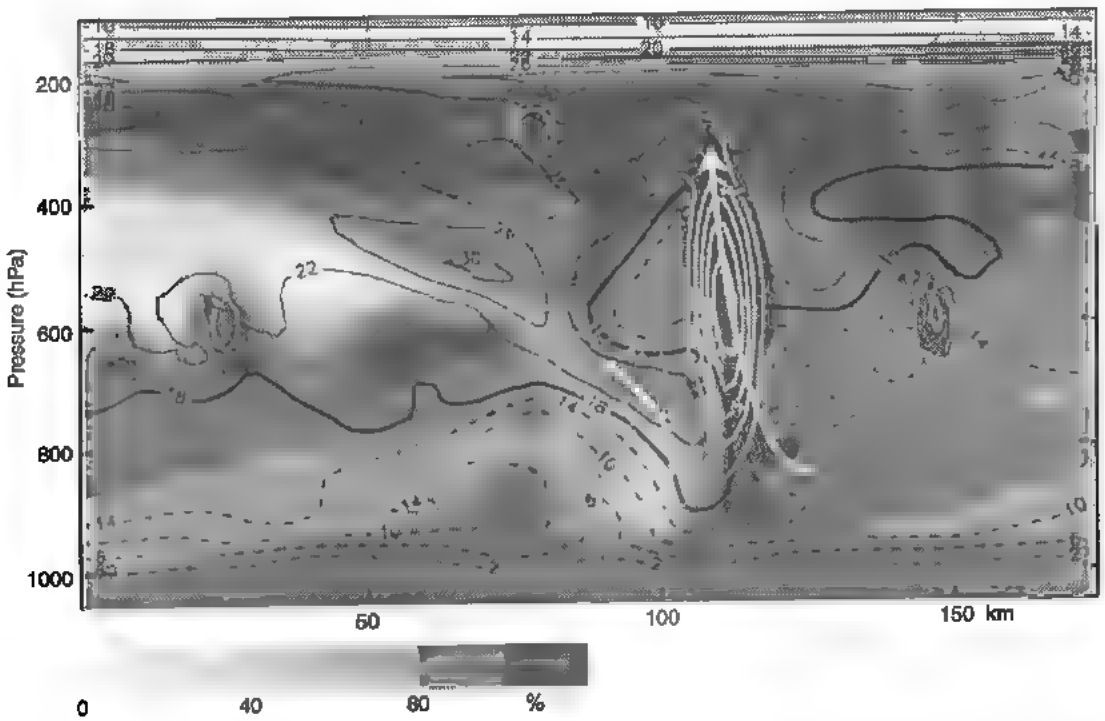

Figure 24. Squall line at 00UTC 3/7/99 from the ND 12 hour forecast at 4km resolution with no convection scheme. Cross section along the line shown in Figure 23. Shading is relative humidity (with respect to ice). Black contours show the wind speed along the section. The thick black 18 m/s contour is the speed of the squall line – dashed contours indicate wind speeds for air flowing from right to left relative to the squall line, continuous contours are for flow from left to right relative to the squall line. White contours are vertical velocity at 1m/s intervals, dashed for descent (0 m/s not included).

The rainfall at 00UTC from the ND 12km run is shown in Figure 25 with the rainfall from the 4 and 2km runs averaged to 12km for comparison. The 12km run did run successfully for the full 12 hours without the convection scheme and produced a reasonable forecast. The precipitation was not as organised as at higher resolution and extended further south with a poor forecast of heavy rain over NE France in the same region where the convective rainbands developed in the runs with the convection scheme. Why storm cells developed over NE France in the 12km run only is an interesting question; maybe the instability was present there in all the runs but couldn't be maintained at 12km, or maybe the higher resolution runs had a somewhat different evolution of the larger-scale flow which generated less instability in that region.

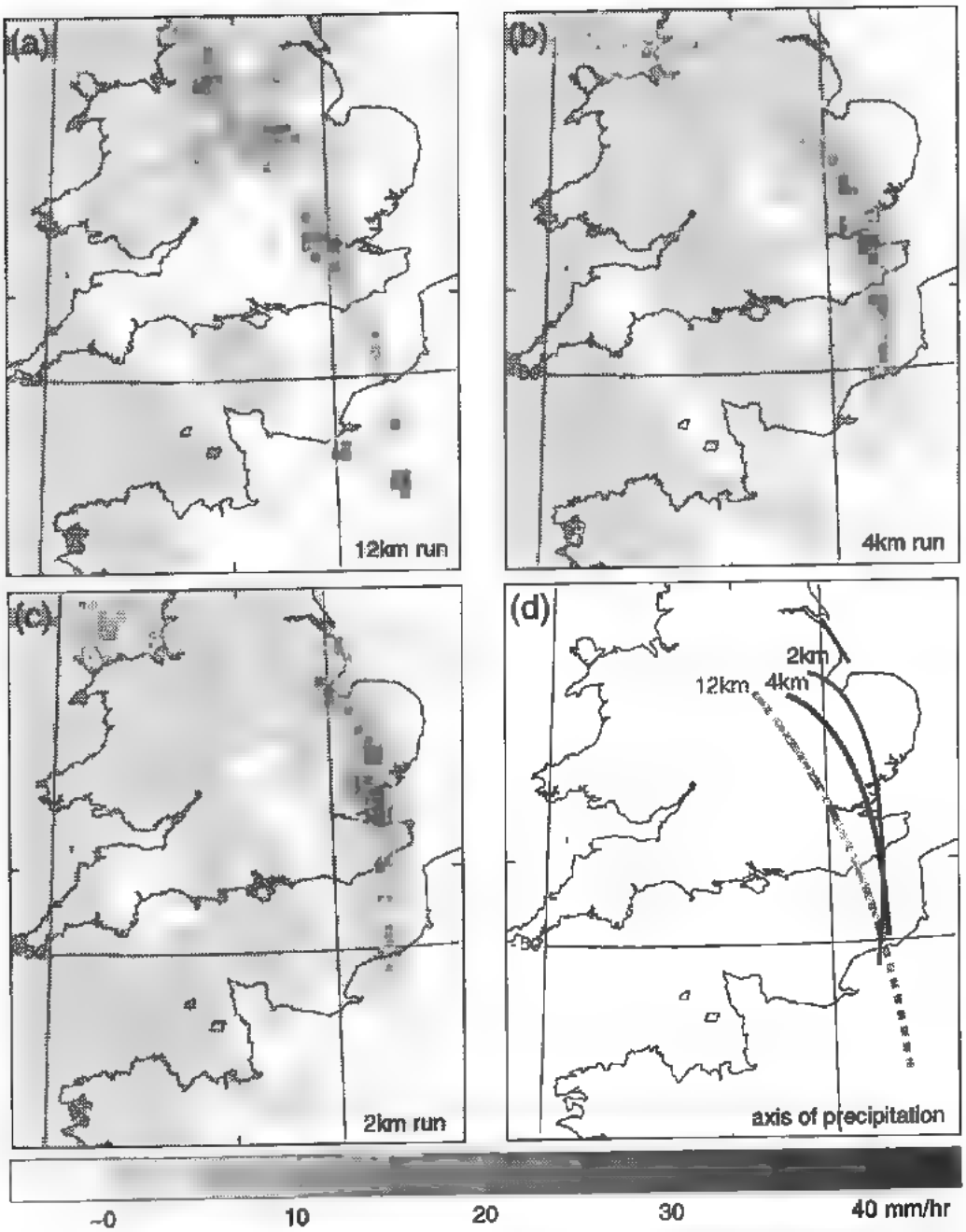

Figure 25. (a), (b) and (c) The precipitation rates at 00UTC 3/7/99 from 12, 4 and 2km resolution ND runs starting at 15UTC 2/7/99 with the convection scheme switched off. The 4 and 2km rain rates have been averaged to 12km resolution to give a like for like comparison. (d) The lines show the axis of the 12, 4 and 2km rainbands from (a), (b) and (c).

The biggest difference between the three simulations at 00UTC was the location of the line of storms. The higher the resolution the further east the band of precipitation occurred (Figure 25d). The rainband positions at 00UTC were different because the propagation speeds through the forecasts were different as shown in Figure 26.

The 4km and 2km runs propagated the squall line at roughly the same speed as the observed event, but the 12km run was much slower (as were all the runs with the convection scheme and short CCT). The shape of the precipitation band also became more curved with increasing resolution and tended to develop further north. This may indicate a different evolution of the larger-scale flow pattern with varying resolution, but that is speculative at this stage.

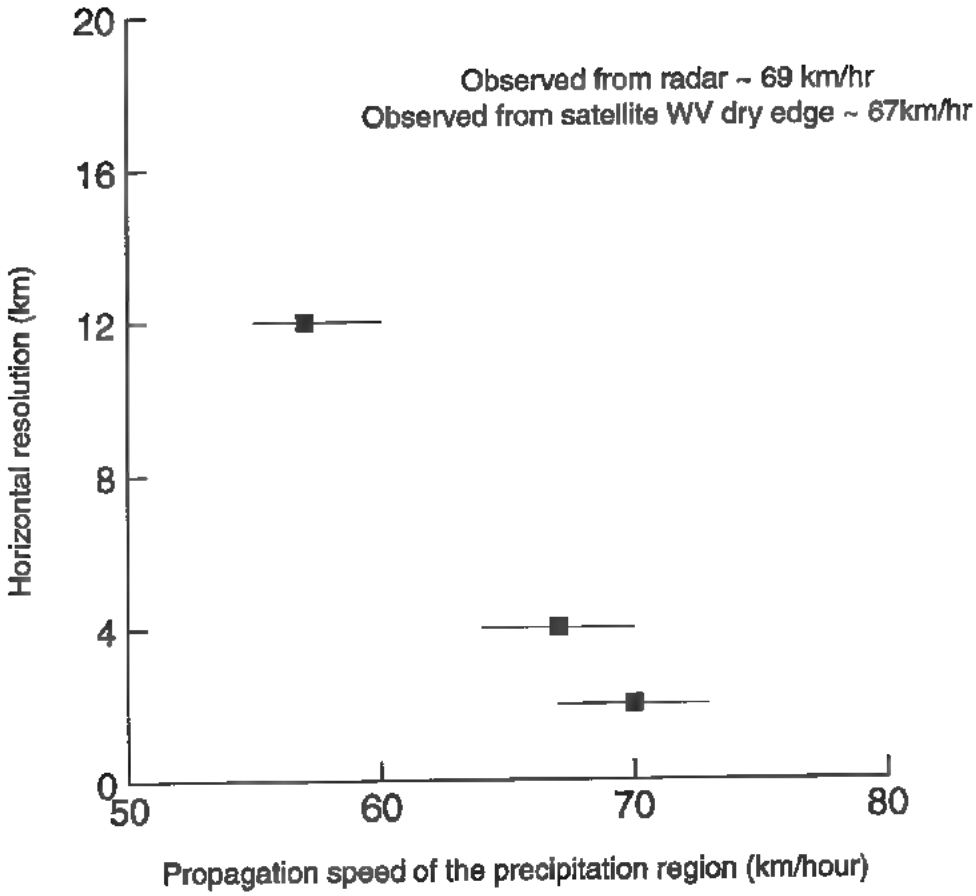

Figure 26. A graph of the propagation speeds of the northern part of the rainband against resolution for the runs with the convection scheme switched off.

The storms were initiated much later at 18.10 2/7/99 in the 12km run compared with 16.50 in the 4km run and 16.40 in the 2km run.

9.1 Summary of this section

- The 2, 4 and 12km resolution New Dynamics simulations all ran successfully without the convection scheme switched on and produced reasonable/good forecasts.
- The simulated rainbands crossed the UK around 2-3 hours ahead of the real event, probably because the mid-level frontal zone in the initial fields was more advanced than in reality.
- The 2 and 4km runs developed a squall-line structure similar to that observed in the radar.
- The storms propagated more quickly and were more intense than in the equivalent runs with the convection scheme switched on.
- The propagation speed of the line of storms increased with higher resolution.
- At 2km and 4km resolution the storms initiated at roughly the same time, but at 12km resolution the initiation time was 1.5 hours later.
- The 2km and 4km forecasts were similar and good in terms of structure and intensity; the 12km simulation was poorer.
- The evolution and propagation speed of the mid-level frontal zone needs to be determined in all the simulations before being able to decide on the best forecast. This includes the runs with the convection scheme. See next section.

10. Meteorological assessment of forecast performance

In this section the various ND runs are examined in the context of what is known about the actual event to try and pick out the best forecast(s). Three aspects are briefly looked into; the propagation speed of the storms, the intensity of the rain and the organisation of the convective system.

10.1 Propagation speed of the storms

The location of precipitation at any given time varied from run to run, as did the propagation speed of the rain area. The propagation speed of the storms increased when the CCT was lengthened, the convection scheme was switched off or the horizontal resolution was increased. Since the observed storms travelled at the same speed as the upper-level dry edge in the WV imagery, it was hoped that the simulated storms would travel at the same speed as the simulated dry intrusion and the relationship between the two would look physically sensible. To highlight the differences in behaviour in this regard, fields from two of the 4km resolution runs will shown here; one with the convection scheme and a 30-minute CCT (discussed in sections 6 & 7) and the other with the convection scheme switched off (discussed in section 9).

A dry intrusion could be clearly identified in both the ND model runs as a layer of air between 400 and 700hPa with relative humidities of below 40% (Figure 28). The propagation speed was found by tracking the region with values below 40% on the 320K isentropic surface (Figure 27). This surface was chosen because it was located in the middle of the dry intrusion. An isentropic surface rather than a pressure or model level was used because dry-intrusion air should maintain a constant potential temperature. The propagation speed was found to be 70km/hour for both runs (Table 3). Figure 27 shows that the rain area was progressing at roughly the same speed as the dry intrusion in the run with the convection scheme switched off (c & d), but in the simulation with the convection scheme running the dry intrusion was catching up with the rain (a & b). This is demonstrated more clearly in the Figure 28 cross sections. The main region of ascent has advanced further along the section in (d) compared to (b). Both runs triggered convection at the leading edge of the dry intrusion, but whether the convection was maintained at the leading edge is difficult to determine because any moist ascent eroded the dry air. Analysis of several cross-sections at hourly intervals combined with the comparison of propagation speeds strongly suggests that the storms did remain largely at the leading edge of the dry intrusion in the run without the convection scheme. This was not so in the run with the convection scheme, where the ascent punctured the dry air behind its leading edge. The labelling in Figure 28 of the updraught U and the edge of the dry intrusion E highlights this difference between the two runs.

If it is correct to assume that the convection should remain at the leading edge of the dry intrusion (evidence from this case and other studies of forward sloping frontal events suggest that it is a good assumption), then in this respect, the run with the convection scheme switched off was the most realistic. The 12km and 2km resolution runs can be assessed by examining the list of propagation speeds in Table 3. Of the simulations discussed in this report, the propagation speed of the storms matched the dry-intrusion speed best in the 2km run without the convection scheme followed closely by the 2km run with a 2-hour CCT and the 4km run without the convection scheme.

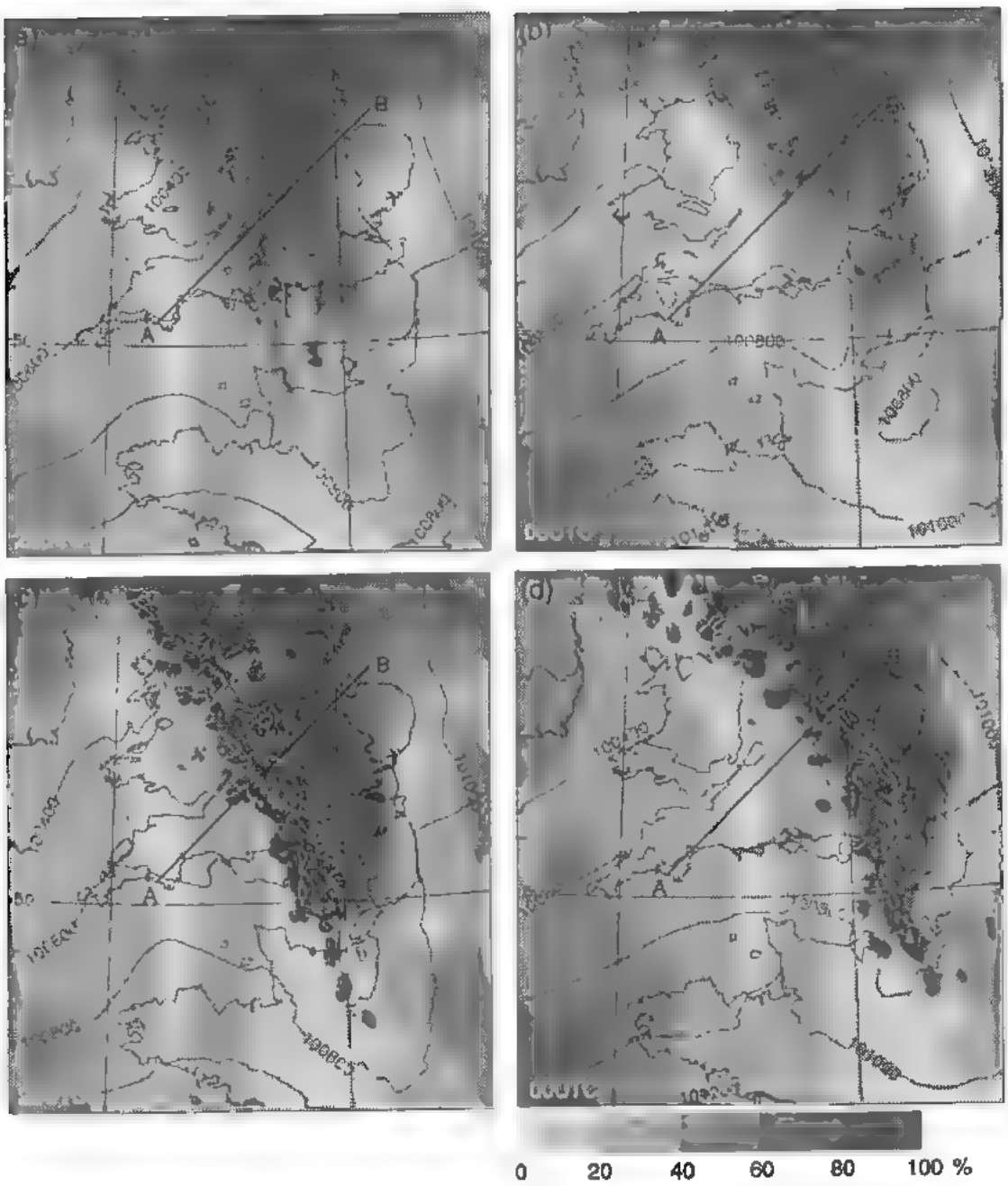

Figure 27. Fields at 22UTC 2/7/99 and 00UTC 3/7/99 from two 4km-resolution ND forecasts starting at 15UTC 2/7/99. Shading is the relative humidity on the 320K isentropic surface (around 500hPa); black contours are surface pressure (Pa); white contours are dynamic precipitation of 5mm/hour. The line AB marks the cross-section in Figure 28. (a) and (b) show the run with the convection scheme running and a CCT of 30 minutes. The dashed white line in (b) shows the position of the band of low relative humidity in (a) labelled D with an arrow to indicate the direction of movement. (c) and (d) shows the run with the convection scheme switched off.

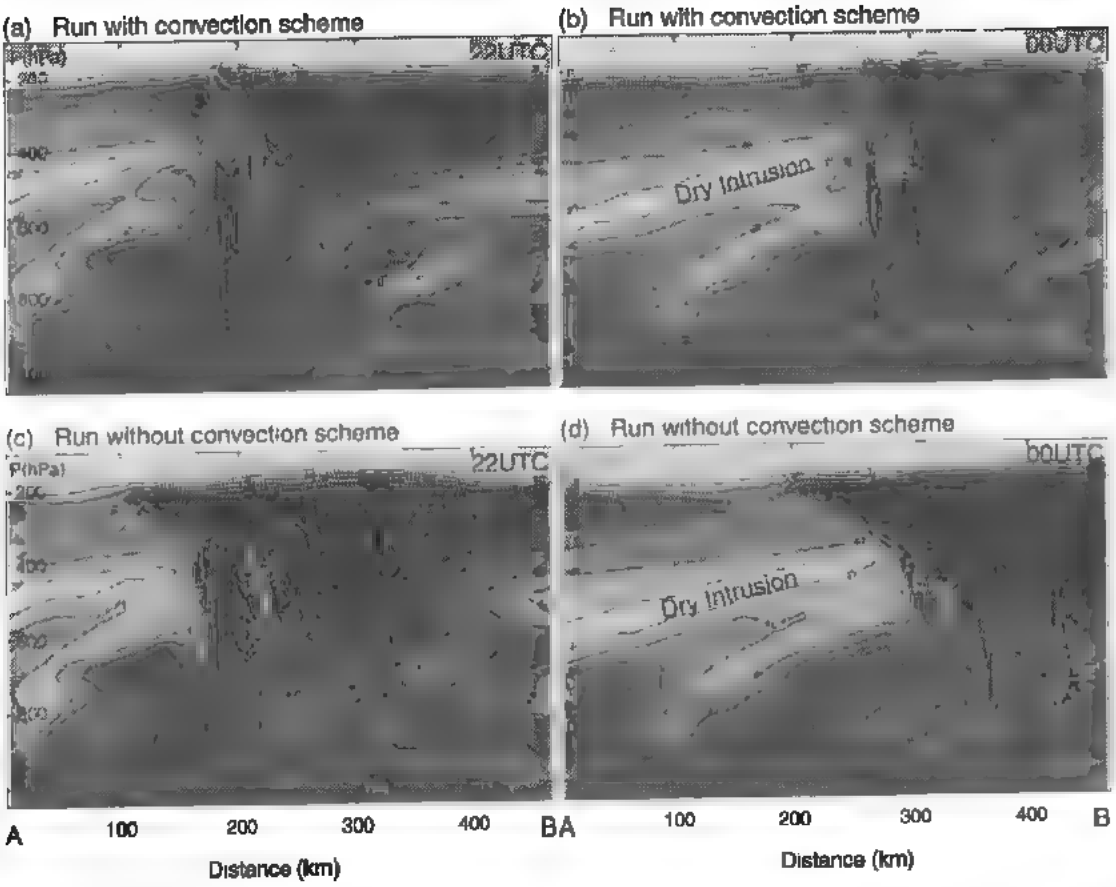

Figure 28. Cross sections along the line AB in Figure 27 at 22UTC 2/7/99 and 00UTC 3/7/99 from the two 4km resolution ND runs shown in Figure 27. Shading is relative humidity; white contours show vertical velocity of 0.5 and 4m/s. The letter E marks the edge of the dry air (dry intrusion); the letter U marks the base of the main updraught. (a) and (b) show the run with the convection scheme running and a CCT of 30 minutes. (c) and (d) show the run with the convection scheme switched off.

ND model runs or observed	Propagation speed of the rain area (km/hr)	Propagation speed of the dry intrusion (km/hr)
12km resolution, convection scheme ON, 30 minutes CCT	41 +/- 6	69 +/- 4
12km resolution, convection scheme ON, 2 hour CCT	52 +/- 4	N/A
12km resolution, convection scheme OFF	57 +/- 3	69 +/- 3
4km resolution, convection scheme ON, 30 minutes CCT	55 +/- 5	70 +/- 3
4km resolution, convection scheme ON, 2 hour CCT	62 +/- 5	N/A
4km resolution, convection scheme OFF	67 +/- 3	70 +/- 3
2km resolution, convection scheme ON, 30 minutes CCT	59 +/- 6	70 +/- 3
2km resolution, convection scheme ON, 2 hour CCT	68 +/- 6	N/A
2km resolution, convection scheme OFF	70 +/- 3	70 +/- 3
Observed	67 +/- 3	68 +/- 4

Table 3

10.2 Peak rainfall intensity

The peak rainfall rates are shown in Table 4 for a selection of the ND runs along with the maximum rate observed at the Reading University field site. The rain rates of over 100 and even 200mm/hour from the 4km and 2km simulations may have seemed far to large if it wasn't for such a high observed value. There is a sampling problem here – it is not surprising that the 2km resolution peak rates are higher than that observed because they are taken from instantaneous values at every gridpoint rather than from just a single observation.

ND model runs or observed	Peak rain rate between 21UTC 2/7/99 & 00UTC 3/7/99 (mm/hr)
12km resolution, convection scheme ON, 30 minutes CCT	20 *
12km resolution, convection scheme ON, 2 hour CCT	43 *
12km resolution, convection scheme OFF	71
4km resolution, convection scheme ON, 30 minutes CCT	103
4km resolution, convection scheme ON, 2 hour CCT	143
4km resolution, convection scheme OFF	167
2km resolution, convection scheme ON, 30 minutes CCT	136
2km resolution, convection scheme ON, 2 hour CCT	256
2km resolution, convection scheme OFF	213
Observed at Reading from tilting siphon rain gauge	160 +/- 50

* Value from only 21 and 00UTC rather than from 10-minute sampling

Table 4

The 2km peak rates therefore appear to be plausible and could provide very useful predictive information about the kind of extreme downpours that may occur in a convective situation. It is curious that the 2km run with a CCT of 2 hours had a higher peak rate than the run without the convection scheme. This when the trend at the lower resolutions was for the runs with the convection scheme switched off to have the higher rates.

A comparison of the distribution of the highest rain rates from the 2km and 4km runs without the convection scheme is shown in Figure 29. The 2km run, as expected, had a larger number of 40x40km squares containing the heavier rain rates, but also moved the risk of heavier precipitation over 100km further north. The 2km run validated better in this regard against observations. This kind of picture is a way of extracting the high resolution information about rainfall intensity, knowing that that each individual storm cell is unlikely to be correct, but that the time and space averaged forecast may be reasonable.

The highest 500hPa vertical velocities at 21 and 00UTC were 7.7m/s (at 12km resolution), 13.3m/s (4km) and 15.8m/s (2km); all from the runs with the convection scheme switched off. These values are large, but since the rainfall rates seemed plausible and high values are expected in severe convective storms they are probably reasonable. The CFL numbers for the highest vertical velocities at each resolution and the 2-minute timestep are 2.6 (12km), 4.7 (4km) and 5.7 (2km). These values are large, indicating that a 1 minute timestep or shorter would be more appropriate for simulating deep convective events at high resolution.

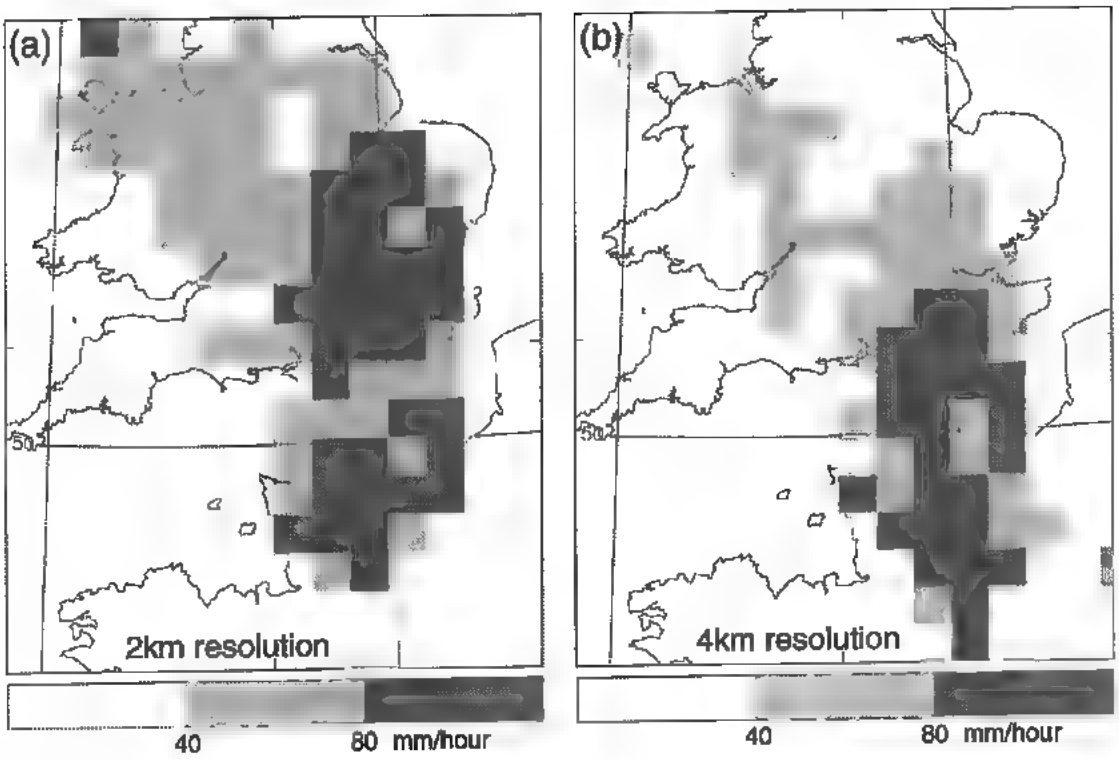

Figure 29. (a) 2km and (b) 4km resolution ND runs with the convection scheme switched off starting at 15UTC. Maximum precipitation rates to occur in 40x40km squares in the period 21UTC 2/7/99 to 00UTC 3/7/99 sampling at 10-minute intervals.

10.3 The organisation of the storms

One of the main differences between the various ND runs was the degree of organisation of the rainband. Switching off the convection scheme or running the convection scheme with long CCTs produced a more linear rainfall distribution. The observed precipitation was less linear and had two separate precipitation areas; the southern one developed into a squall line. The reason why two separate rain areas developed is not known, but a strong possibility is that it was associated with a multiplicity in the pre-existing mesoscale structure. A clue that this may have been the case is that the model runs did have evidence of a double structure in the dry intrusion (Figures 27 & 28). If this was important then it means that there is a necessity for high-resolution models to have this kind of subtle mesoscale detail in the initial fields if individual storms are to be predicted correctly.
The fact that the high-resolution simulations developed a squall line is encouraging (Figures 22-24). Again, it is the 2km run without the convection scheme that is regarded as being the best. Despite not having the two separate storm areas, it was the best forecast given the larger-scale forcing dynamics. The 4km run without the convection scheme was nearly as good.

11. Conclusions

Simulations of an organised convective event have been successfully run using the New Dynamics at 12, 4 and 2km resolution. The forecasts were generally good. Increased resolution produced better forecasts of the propagation speed, location, structure and intensity of the convective system.

The forecasts were very sensitive to changes in the length of the CAPE closure timescale in the convection scheme at all resolutions. Both the distribution, propagation speed and intensity of rainfall were strongly affected, but the combined convective and dynamic precipitation rates averaged over the area of the 2km resolution domain remained nearly constant.

Rapidly propagating bands of precipitation from the convection scheme developed in all the runs in which the CAPE closure timescale was sufficiently short. This was around 30 minutes or less at 12km and 2km resolution and 1 hour or less at 4km resolution. These bands were not observed in reality and acted to make the forecasts worse by retarding and weakening the main area of precipitation as well as initiating dynamic precipitation in places. The probable mechanism was a coupling between the convection scheme and the dynamics. Temperature increments from the convection scheme lead to vertical motion in the dynamics which in turn triggered the convection scheme.

Changing the length of the timestep in the 4km resolution simulation with a CAPE closure timescale of 30 minutes had a big impact on the evolution of the dynamic precipitation, but little effect on the propagating convective rainbands. The average dynamic/convective rain rate decreased/increased with lengthening timestep, but the total remained nearly constant. The run failed with a 4-minute timestep; seemingly because the diffusion became unstable.

The simulations without the convection scheme all ran successfully, even at 12km resolution. As the resolution was increased the propagation speed of the rain area increased. The 2km and 4km resolution runs produced better forecasts than any of the runs with the convection scheme. At these resolutions the rain area became organised into a squall line like structure similar to that observed by the radar. The 12km resolution forecast without the convection scheme was reasonable but not an improvement on the 12km run with the convection scheme using a CAPE closure timescale of 2 hours.

The forecast that validated best against observations was the 2km run without the convection scheme. The propagation speed of the rain was close to the propagation speed of the dry intrusion and developed on the leading edge of the dry intrusion. The rainfall intensities were high but plausible. A squall line structure developed and the precipitation was better placed by developing further north than the lower resolution runs.

Although the 2km run without the convection scheme was the best, the 4km run without the convection scheme was not much poorer and could be regarded as the best value simulation as it captured nearly all the 2km detail but used less computer time and memory.

11.1 Future work

Further cases studies are required to see if the results obtained here are general. Several cases will provide statistics to back up performance assessments. This case study was done without the capability of data assimilation in the New Dynamics, future work will need to incorporate data assimilation experiments into the high-resolution modelling assessment. At 4km resolution or higher the convective event studied here was simulated best without running the convection scheme, however this might not be the case for less intense

events. This will require investigation and perhaps points to the potential benefits of using a shallow convection scheme. The relative humidity sensitive closure for the convection scheme should be tried. Case studies should be compared with idealised simulations and used as a basis for idealised initial conditions.

The sensitivity to changing the vertical resolution has not been sufficiently examined and higher vertical resolutions should be tried, especially if going to 1km horizontal resolution. The sensitivity to changing the domain size and the effect of running from a higher resolution limited area domain rather than the global domain also require investigation. Ultimately, the objective is to discover the best configuration for an operational high-resolution forecast system.

11.2 Acknowledgements

I would like to thank the following people: Peter Clark, Humphrey Lean and Richard Forbes for showing me how run the New Dynamics and for valuable discussions; Zoe Gardner for help when the model failed; Clive Jones for help with the ancillary files and Ken Spiers for providing the rain rate measurements from the Reading University field site.

12. References

Browning, K. A., Roberts, N. M. and Sim, C. S., 1996: A mesoscale vortex diagnosed from combined satellite and model data. *Meteorol. Appl.*, 3, 1-4

Gregory, D., Inness, P. and Gregory, J. M., 1999: The convection scheme. *Unified Model Documentation Paper .*, 27

Griffiths, M., Thorpe, A. J. and Browning, K. A., 1998: Convective destabalisation by a tropopause fold diagnosed using potential vorticity inversion. *JCMM internal report.*, 96

Hoskins, B. J., McIntyre, M. E. and Robertson, A. W., 1985: On the use and significance of isentropic potential vorticity maps. *Q. J. Roy. Met. Soc.*, 111, 877-946

Lean, H. W., 2000: Tests of New Dynamics Model on the FASTEX IOP16 case. *JCMM internal report.*, 119. (*NWP Technical Report.*, 320)

Roberts, N. M., 2000: The relationship between water vapour imagery and thunderstorms. *JCMM internal report.*, 110. (*NWP Technical Report.*, 300)

Staniforth, A., White, A. and Wood, N., 2000: New Dynamics Formulation. *Unified Model Documentation Paper .*, 15

Weisman, M. L., Skamarock, W. C. and Klemp, J. B., 1997: The resolution dependence of explicitly modelled convective systems. *Mo. Wea. Rev.*, 125, 527-548

Appendix 1

The grids used

1. 12km resolution (mesoscale model domain)

146 x 182 points
Grid length 0.11 x 0.11 degrees
Latitude of rotated north pole 37.5 degrees
Longitude of rotated north pole 177.5 degrees
Bottom left rotated latitude -8.41 degrees
Left edge rotated longitude 352.95 degrees
(Top left rotated latitude 11.5 degrees)

2. 4km resolution

190 x 210 points
Grid length 0.035 x 0.035 degrees
Latitude of rotated north pole 37.5 degrees
Longitude of rotated north pole 177.5 degrees
Bottom left rotated latitude -5.315 degrees
Left edge rotated longitude 357.0 degrees
(Top left rotated latitude 2.0 degrees)

3. 2km resolution

280 x 340 points
Grid length 0.018 x 0.018 degrees
Latitude of rotated north pole 37.5 degrees
Longitude of rotated north pole 177.5 degrees
Bottom left rotated latitude -4.602 degrees
Left edge rotated longitude 358.0 degrees
(Top left rotated latitude 1.5 degrees)

Appendix 2

Parameters common to all the runs at a particular resolution

12km resolution

Ran on t3ea, New Dynamics version 3.0
45 levels, 17 boundary layer levels
Boundary updating every 3 hours, using merged orography
Timestep 5 minutes (unless stated otherwise), radiation timestep 1 hour
Ancillary files from ancillary creation version 5.0
Diffusion – none except at top level(s)
Physics from UM version 5, Boundary layer version 6A, Precipitation scheme 3A
Radiation 3A, Hydrology 5A
Convection option 3, Convective momentum flux off
Boundary updating every 3 hours from ND global 45 level run with a CAPE closure timescale of 2 hours
User CPU time 136600 seconds on 64 processors – Approx run time 40 minutes
Allocated memory – 60Mw per processor

4km resolution

Ran on t3ea, New Dynamics version 3.0 (older runs version 2.9)
45 levels, 17 boundary layer levels
Boundary updating every 1 hour, using merged orography
Timestep 2 minutes (unless stated otherwise), radiation timestep 20 minutes
Ancillary files from ancillary creation version 5.0
Diffusion - del 4, coefficient 6.8e3 (order 1 at top level) for U,V, T and W
Physics from UM version 5, Boundary layer version 6A, Precipitation scheme 3A
Radiation 3A, Hydrology 5A
Convection option 3, Convective momentum flux off
Boundary updating every hour from the 12km resolution 45 level run with a CAPE closure timescale of 30 minutes
User CPU time 261200 seconds on 64 processors – Approx run time 1 hour 10 minutes
Allocated memory - 60Mw per processor

2km resolution

Ran on t3ea, New Dynamics version 3.0
45 levels, 17 boundary layer levels
Boundary updating every 1 hour, using merged orography
Timestep 1 minute, radiation timestep 20 minutes
Ancillary files from ancillary creation version 5.0
Diffusion - del 4, coefficient 6.8e3 (order 1 at top level) for U,V, T and W
Physics from UM version 5, Boundary layer version 6A, Precipitation scheme 3A
Radiation 3A, Hydrology 5A
Convection option 3, Convective momentum flux off
Boundary updating every hour from the 4km resolution 45 level run with a CAPE closure timescale of 30 minutes
User CPU time 1494200 seconds on 96 processors – Approx run time 4 hours 20 minutes
Allocated memory – 70Mw per processor

CURRENT JCMM INTERNAL REPORTS

This series of JCMM Internal Reports, initiated in 1993, contains unpublished reports and also versions of articles submitted for publication. The complete set of Internal Reports is available from the National Meteorological Library on loan, if required.

1. **Research strategy and programme**
   K A Browning et al
   January 1993

2. **The GEWEX Cloud System Study (GCSS)**
   GEWEX Cloud System Science Team
   January 1993

3. **Evolution of a mesoscale upper tropospheric vorticity maximum and comma cloud from a cloud-free two dimensional potential vorticity anomaly**
   K A Browning
   January 1993

4. **The global energy and water cycle**
   K A Browning
   July 1993

5. **Structure of a midlatitude cyclone before occlusion**
   K A Browning and N Roberts
   July 1993

6. **Developments in systems and tools for weather forecasting**
   K A Browning and G Szejwach
   July 1993

7. **Diagnostic study of a narrow cold frontal rainband and severe winds associated with a stratospheric intrusion**
   K A Browning and R Reynolds
   August 1993

8. **Survey of perceived priority issues in the parametrizations of cloud-related processes in GCMs**
   K A Browning
   September 1993

9. **The effect of rain on longwave radiation**
   I Dharssi
   September 1993

10. **Cloud microphysical processes - a description of the parametrization used in the large eddy model**
    H Swann
    October 1993

11. **An appreciation of the meteorological research of Ernst Kleinschmidt**
    A J Thorpe
    May 1992

12. **Potential vorticity of flow along the Alps**
    A J Thorpe, H Volkert and Dietrich Heimann
    August 1992

13. **The representation of fronts**
    A J Thorpe
    January 1993

14. **A parametrization scheme for symmetric instability: test for an idealised flow**
C S Chan and A J Thorpe
February 1993

15. **The Fronts 92 Experiment: a Quicklook Atlas**
Edited by T D Hewson
November 1993

16. **Frontal wave stability during moist deformation frontogenesis**
Part 1: Linear wave dynamics
C H Bishop and A J Thorpe
May 1993

17. **Frontal wave stability during moist deformation frontogenesis**
Part 2. The suppression of non-linear wave development
C H Bishop and A J Thorpe
May 1993

18. **Gravity waves in sheared ducts**
S Monserrat and A J Thorpe
October 1993

19. **Potential vorticity and the electrostatics analogy: quasi-geostrophic theory**
C Bishop and A J Thorpe
November 1993

20. **Recent advances in the measurement of precipitation by radar**
A J Illingworth
April 1993

21. **Micro-physique et givrage: cloud microphysics and aircraft icing**
A J Illingworth
May 1993

22. **Differential phase measurements of precipitation**
M Blackman and A J Illingworth
May 1993

23. **Estimation of effective radius of cloud particles from the radar reflectivity**
N I Fox and A J Illingworth
May 1993

24. **A simple method of Dopplerising a pulsed magnetron radar**
A Hua, A J Illingworth and J Eastment
November 1993

25. **Radiation and polar lows**
George C Craig
February 1994

26. **Collected preprints submitted to the International Symposium on the Life Cycles of Extratropical Cyclones; Bergen, Norway, 27 June - 1 July 1994**
April 1994

27. **Convective frontogenesis**
Douglas J Parker and Alan J Thorpe
April 1994

28. **Improved measurement of the ice water content in cirrus using a total water evaporator**
Philip R A Brown and Peter N Francis
April 1994

29. **Mesoscale effects of a dry intrusion within a vigorous cyclone**
K A Browning and B W Golding
April 1994

30. **GEWEX Cloud System Study, Science Plan**
May 1994

31. **Parametrization of momentum transport by convectively generated gravity waves**
R Kershaw
May 1994

32. **Mesoscale Modelling Newsletter No 5**
May 1994

33. **Observations of the mesoscale sub-structure in the cold air of a developing frontal cyclone**
K A Browning, S A Clough, C S A Davitt, N M Roberts and T D Hewson
May 1994

34. **Longwave radiative forcing of a simulated tropical squall line**
Imtiaz Dharssi
July 1994

35. **On the nature of the convective circulation at a kata-cold front**
K A Browning
September 1994

36. **Collective preprints of papers submitted to the COST-75 International Seminar on Advanced Weather Radar Systems, Brussels, 20-23 September 1994**
November 1994

37. **Use of satellite imagery to diagnose events leading to frontal thunderstorms: Parts I and II of a case study**
K A Browning and N M Roberts
November 1994

38. **The role of spaceborne millimetre-wave radar in the global monitoring of ice cloud**
P R A Brown, A J Illingworth, A J Heymsfield, G M McFarquhar, K A Browning and M Gosset
December 1994

39. **Potential vorticity inversion**
Michal Ziemianski
October 1994

40. **Theory of mature tropical cyclones; a comparison between Kleinschmidt (1951) and Emanuel (1986)**
Suzanne L Gray
December 1994

41. **Dispersion and removal of pollutants during the passage of an atmospheric frontal system**
N R Gimson
December 1994

42. **The role of snow sublimation in frontogenesis**
D J Parker and A J Thorpe
December 1994

43. **Potential vorticity and the electrostatics Analogy: Ertel-Rossby formulation**
A J Thorpe and C H Bishop
December 1994

44. **Mesoscale aspect of extratropical cyclones: an observational perspective**
K A Browning
January 1995

45. **A polar low outbreak: evolution and mesoscale structures**
T D Hewson, G C Craig and C Claud
February 1995

46. **Generation of near-surface gusts of deep convection**
K Nakamura and R Kershaw
April 1995

47. **Attribution concepts applied to the Omega Equation**
S A Clough, C S A Davitt and A J Thorpe
June 1995

48. **Parametrization of mixed-phase cloud and precipitation**
Susan P Ballard and M Gerard Hutchinson
June 1995

49. **Short-range forecasting of stratocumulus: initialization prediction**
Susan P Ballard, Simon D Jackson and B Macpherson
June 1995

50. **Contributions of the JCMM/Dept of Meteorology Radar Group to the 27th AMS Radar Meteorology Conference, Vail October 1995**
June 1995

51. **Cold pools in shear**
Douglas J Parker
September 1995

52. **High-resolution analysis of frontal fracture**
K A Browning, S P Ballard and C S A Davitt
September 1995

53. **The albedo of broken cloud fields: calculations using a modified two stream radiation code**
Imtiaz Dharssi and Roy Kershaw
October 1995

54. **Parametrization of momentum transport by convection. I: theory and cloud modelling results**
R Kershaw and D Gregory
November 1995

55. **Variation of frontal structure along a cold front**
K A Browning and N M Roberts
November 1995

56. **Secondary frontal waves**
Douglas Parker
December 1995

57. **Objective fronts**
T D Hewson
March 1996

58. **Mesoscale analysis of the activation of a cold front during cyclogenesis**
K A Browning, N M Roberts and A J Illingworth
June 1996

59. **Investigation of different representations of rain in a 1-d evaporation model**
H Swann
May 1996

60. **Parametrization of diabatic processes in the inversion of the omega-equation**
M Athanassiadou and A J Thorpe
June 1996

61. **The role of the environmental flow in the development of secondary frontal cyclones**
I A Renfrew, A J Thorpe and A Joly
June 1996

62. **Consequences of the geostrophic momentum approximation on barotropic instability**
S Malardel, A J Thorpe and A Joly
June 1996

63. **Contributions to the AMS/RMS Conference on Mesoscale Processes**
Reading, 9-13 September 1996

64. **Vorticity and potential vorticity in stratified flows interacting with an isolated obstacle**
Jorge A Gutiérrez and A J Thorpe
September 1996

65. **Triple point development: two case studies**
Douglas Parker
September 1996

66. **Radar observations of wind-shear splitting within evolving atmospheric Kelvin-Helmholtz billows**
D Chapman and K A Browning
April 1997

67. **Cold frontal structure derived from radar wind profilers**
K A Browning, D Jerrett, J Nash, T Oakley and N M Roberts
May 1997

68. **The dry intrusion and its effect on the frontal, cloud and precipitation structure of extratropical cyclones**
K A Browning - Text of invited special lecture at the Spring Conference
of the Meteorological Society of Japan, University of Tsukuba, 22 May 1997

69. **Met. Office Unified Model data, diagnostics, graphics programs, and other observational data available from the JCMM through the aegis of the Universities Weather Research Network (UWERN).** (Plus supplement)
Peter Panagi and Ed Dicks
June 1997

70. **Contributions of the JCMM/Dept of Meteorology Radar Group to the 28th AMS Radar Meteorology Conference.** Austin, Texas
September 1997

71. **Sensitivity of short-range weather forecasts to local potential vorticity modifications**
Meral Demi tas and Alan Thorpe
July 1997

72. **Objective identification of frontal wave cyclones**
T D Hewson
August 1997

73. **Attribution and its application to mesoscale structure associated with tropopause folds**
A J Thorpe
September 1997

74. **The role of the environmental flow in the development of secondary frontal cyclones**
Ian A Renfrew, Alan J Thorpe and Craig H Bishop
September 1997

75. **Potential vorticity: a short history of its definitions and uses**
Alan J Thorpe and Hans Volkert
September 1997

76. **Superposing semi-geostrophic potential vorticity anomalies**
H R Birkett and A J Thorpe
September 1997

77. **Short period forecasting of catchment-scale precipitation.**
Part 1: the role of Numerical Weather Prediction
M A Pedder, M Haile and A J Thorpe
September 1997

78. **Verification of the tracking technique used in an experimental cloud motion wind inferring system**
Z Wang, K A Browning and G A Kelly
October 1997

79. **A preliminary study of Fourier series analysis for cloud tracking with GOES high temporal resolution images**
Z Wang
October 1997

80. **Analysis of an ex-tropical cyclone after reintensifying as a warm-core extratropical cyclone**
K A Browning, G Vaughan and P Panagi
November 1997

81. **A JCMM overview of FASTEX IOPs**
S A Clough, H W Lean, N M Roberts, H Birkett, J-P Chaboureau, R Dixon, M Griffiths, T D Hewson and A Montani
January 1998

82. **Programs for PV inversion and modification**
Meral Demirtas
December 1997

83. **Release of potential shearing instability in warm frontal zones**
D Chapman and K A Browning
February 1998

84. **The European Cloud-Resolving Modelling Programme (EUCREM)**
Summary Report from the coordinator
P W White
April 1998

85. **A frontal wave database**
T D Hewson
April 1998

86. **Layering observed in dropsoundings from IOP 1 of Fronts 92**
S A Clough
May 1998

87. **Use of wind-shear displays for Doppler radar data**
D Chapman and K A Browning
May 1998

88. **Radar estimates of rainfall rates at the ground in bright band and non-bright band events**
T J Smyth and A J Illingworth
June 1998

89. **Correction for attenuation of radar reflectivity using polarisation data**
T J Smyth and A J Illingworth
June 1998

90. **The effects of convection on chemical reactions and precipitation scavenging**
Neil R Gimson
July 1998

91. **How to use the display program DISP**
Nigel Roberts
August 1998

92. **Conceptual models of cyclogenesis**
Adrian T Semple
August 1998

93. **Observations of oblate hail using dual polarisation radar and implications for hail detection schemes**
T J Smyth, T M Blackman and A J Illingworth
September 1998

94. **The semigeostrophic diagnosis of vertical motion. Part I: Formulation and co-ordinate transformations**
Mike A Pedder and Alan J Thorpe
September 1998

95. **The semigeostrophic diagnosis of vertical motion. Part II: Results for an idealised baroclinic wave life cycle**
Alan J Thorpe and Mike A Pedder
September 1998

96. **Convective destabilisation by a tropopause fold diagnosed using potential vorticity inversion**
Morwenna Griffiths, Alan Thorpe and Keith Browning
October 1998

97. **Forecast skill of the ECMWF model using targeted observations during FASTEX**
A Montani, A J Thorpe, R Buizza and P Unden
October 1998

98. **Observations and model simulations of the FASTEX IOP 16 frontal wave - effects of sublimation**
Sid A Clough, Humphrey W Lean, Nigel M Roberts and Richard M Forbes
December 1998

99. **The application of conceptual models in NWP**
Adrian T Semple
January 1999

100. **Mesoscale analysis of arc rainbands in a dry slot**
K A Browning and N M Roberts
January 1999

101. **Interaction of mesoscale tropopause depressions with a warm-core cyclone: observational and model analyses, and sensitivity to analysis errors**
K A Browning, A J Thorpe, A Montani, D Parsons, M Griffiths, P Panagi and E M Dicks
February 1999

102. **The use of water vapour imagery and PV inversion to adjust initial conditions in NWP**
Sean J Swarbrick
February 1999
This report is no longer available; see Internal Report No.108

103. **Summary notes for a lecture course on Waves in the Atmosphere and Ocean**
A A White
March 1999

104. **Results of a questionnaire on the operational value of conceptual models (CMs) of fronts and cyclones**
N M Roberts & M V Young
July 1999

105. **Contributions to the Poster Session at the 1998 UWERN Annual Science Meeting**
assembled by A A White
August 1999

106. **The objective analysis of dropsonde data from FASTEX**
Richard Forbes, Sid Clough, Mark Dixon, Andy Macallan & Nigel Roberts
January 2000

107. *NWP Technical Report No.302*
Implications for Mesoscale Modelling from a Study of the FASTEX IOP 16 Mid-latitude Cyclone
Richard M Forbes, Humphrey W Lean, Nigel M Roberts and Peter A Clark
March 2000

108. *NWP Technical Report No.291*
The use of water vapour imagery and PV inversion to adjust initial conditions in NWP
Final Project Report
Sean J Swarbrick
September 1999

109. *NWP Technical Report No.294*
A guide to aspects of water vapour imagery interpretation: the significance of dry regions
Nigel M Roberts
January 2000

110. *NWP Technical Report No.300*
The relationship between water vapour imagery and thunderstorms
Nigel M Roberts
February 2000

111. *NWP Technical Report No.293*
Holomorphic structures in hydrodynamical models of nearly geostrophic flow
V N Roubtsov and I Roulstone
January 2000

112. *NWP Technical Report No.301*
Multi-sensor synthesis of the mesoscale structure of a cold-air comma cloud system
K A Browning, P Panagi and E M Dicks
March 2000

113. *NWP Technical Report No.307*
Observations of stratospheric air entering the circulation of a polar low
K A Browning and E M Dicks
May 2000

114. *NWP Technical Report No.309*
Wind profiler – Unified Model comparison statistics
Peter Panagi & Ed Dicks
March 2000

115. *NWP Technical Report No.310*
Towards a similarity theory of moist convective updrafts
Olaf Stiller and George C Craig
May 2000

116. *NWP Technical Report No.312*
The mystery of striated cloud heads in satellite imagery
R S Dixon, K A Browning and G J Shutts
April 2000

117. *NWP Technical Report No.313*
MDIAG: a Fortran 90 program to compute diagnostics on pressure levels from Unified Model data on model levels
Peter Panagi
June 2000

118. *NWP Scientific Paper No.56*
Rearrangements of functions with applications to meteorology and ideal fluid flow
R J Douglas
June 2000

119. *NWP Technical Report No.320*
Tests of New Dynamics Model on the FASTEX IOP16 case
Humphrey Lean
September 2000

120. *NWP Scientific Paper 57*
A classification of FASTEX cyclones using a height-attributable QG vertical motion diagnostic
A C L Deveson, K A Browning, T D Hewson
September 2000

121. *NWP Scientific Paper 59*
Measurements of dissipation rate in frontal zones
D.Chapman, K A Browning
August 2000

122. *NWP Technical Report 331*
Not issued yet

123. *NWP Technical Report 337*
A Case Study of High Resolution Fog Forecasts with the New Dynamics
P. Clark
November 2000

124. *NWP Technical Report 338*
Comparison of ECMWF Winter-Season Cloud Fraction with Radar Derived Values
Robin J. Hogan, Christian Jakob, Anthony J. Illingworth
January 2001

125. *NWP Technical Report 339*
Deriving Cloud overlap statistics from radar
Robin J. Hogan, Anthony J. Illingworth
January 2001

126. *NWP Technical Report 344*
Results from simulations of an organised convective event using the New Dynamics at 12, 4 and 2km resolution.
Nigel Roberts
January 2001

Met Office Joint Centre for Mesoscale Meteorology Department of Meteorology
University of Reading PO Box 243 Reading RG6 6BB United Kingdom
Tel: +44 (0)118 931 8425 Fax: +44 (0)118 931 8791
www.metoffice.com